QCD IN HADRON-HADRON COLLISIONS

Michael G. Albrow*
Fermi National Accelerator Laboratory, MS 318
P.O. Box 500, Wilson Road, Batavia, IL 60510

ABSTRACT

Quantum Chromodynamics provides a good description of many aspects of high energy hadron-hadron collisions, and this will be described, along with some aspects that are not yet understood in QCD. Topics include high E_T jet production, direct photon, W, Z, and heavy flavor production, rapidity gaps, and hard diffraction.

*Supported by DOE contract through Fermilab contracts.

1 Quarks and Gluons in Hadrons

In the Standard Model, the strongly interacting particles, or *hadrons*, are composites of the more fundamental quarks q, antiquarks $\bar{q}$, and gluons g. While the hadrons are extended objects with dimensions of order 1 fm (10^{-13} cm), their constituents $q, \bar{q}$, and g, generically called partons,[1] are point-like at all scales presently accessible. With a resolving power of order 10^{-17} cm, reached in hadron-hadron collisions at the Fermilab Tevatron, they still behave like points. However, if you "observe" a proton, by probing it with a photon or any other particle, what you "see" depends very much on the wavelength λ of the probe. If you probe the proton with x-rays ($\lambda \approx 10^{-8}$ cm) you will see a point-like object. If you use photons with a wavelength of about 1 fm, the experiments will show a fuzzy blob [quantified by the electromagnetic form factor $F(Q^2)$, where Q^2 is $(\hbar c)^2\lambda^{-2}$]. If you further decrease the wavelength of the photon (increasing Q^2), you begin to see that the proton is lumpy, and three *valence quarks* become apparent. This was the famous experiment at SLAC in 1969 (for which Friedman, Kendall, and Taylor received the Nobel Prize in 1990), scattering electrons on protons and finding "point-like" structures. As you continue to decrease the wavelength of the photons, the quarks always appear smaller than the resolution, but additional partons appear. The fraction of the proton's momentum carried by quarks and antiquarks decreases as they radiate gluons. Gluons convert into $q\bar{q}$ or gg pairs which in turn can radiate gluons, and we have a branching tree of q and g. The smaller the probe wavelength (the larger the Q^2), the better the resolution, and the more of these low-momentum-fraction partons you observe. This is called *evolution*. Thus, the proton (like all other hadrons) has an ever-changing structure and composition; it just depends how *hard* you look. Larger Q^2 means harder.

What are the quarks and gluons? The quarks are fermions, spin $\frac{1}{2}\hbar$ point-like electric charges. There are six types, called *flavors*, named down (d), up (u), strange (s), charm (c), bottom or beauty (b), and top (t). With the electric charge of the electron defined to be −1, the u, c, and t quarks have charge $+\frac{2}{3}$, and the d, s, and b quarks have charge $-\frac{1}{3}$. The quarks have another kind of charge for the strong, Quantum Chromodynamics or QCD, interaction. This is called a *color* charge by analogy with the fact that three lights (red, green, and blue) together make white (colorless) light.* Quarks are said to be in a color triplet state. At any time a quark can be, with equal probability, in a R, G, or B state. A triplet of quarks, one of each color, makes a colorless composite or hadron, such as a proton. Antiquarks carry anticolor charges: $\bar{R}, \bar{G}$, or $\bar{B}$. Three quark states qqq are called *baryons*, and three antiquarks $\bar{q}\bar{q}\bar{q}$ are antibaryons. Mesons are hadrons consisting primarily of a quark and an antiquark; the color and anticolor (e.g., $R\bar{R}$) cancel to make a colorless composite. Gluons are continually exchanged between the q and $\bar{q}$. Gluons are in color octet states, having a color and an anticolor, e.g., $R\bar{G}$. The "octet" comes from group theory arithmetic:

$$3 \times \bar{3} = 8 + 1$$

The singlet $R\bar{R} + G\bar{G} + B\bar{B}$ decouples from the theory; it is not part of the group $SU(3)$. Exchanged gluons, in the space-like t-channel, having no defined direction of propagation, can be equally $R\bar{G}$ and $G\bar{R}$; these are indistinguishable. The net effect is to change the color of the coupling quarks. In the t-channel we have, e.g., $q_R q_B \rightarrow q_B q_R$. Gluons can also be "exchanged" in the time-like s channel, for $q\bar{q}$ annihilation, and they carry the color of the quark and the anticolor of the antiquark. However, a quark and antiquark of opposite color cannot annihilate into a single gluon; they can, however, annihilate by the electromagnetic or weak interaction into a photon, W, or Z.

The strength of the coupling between quarks and gluons depends on the four-momentum-transfer-squared Q^2 involved in the process and is denoted by $\alpha_S(Q^2)$ to reflect the notation α_{em} of QED. The coupling $\alpha_S(Q^2)$ is large (of order 1) at very small Q^2 (of order 1 GeV^2) and falls with Q^2 to become about 0.12 at $Q^2 = M_Z^2$. The particle Z is the neutral weak intermediate vector boson, with mass 91.19 GeV. Probes of progressively shorter wavelength see the strong interaction becoming weaker, and the quarks and gluons behaving more like free particles. This is known as *asymptotic freedom*. On the other hand at small Q^2, or long wavelengths, the coupling becomes so large that we do not know how to calculate interactions (the *nonperturbative* regime) except by approximating space-time by a discrete set of points and using vast computing power. This is the approach called *Lattice QCD*.

We can in principle make hadronic states out of any colorless composite, hence not only qqq, $\bar{q}\bar{q}\bar{q}$, and $q\bar{q}$, but also gg and ggg. The latter are called *gluonia* and *glueballs* and have resisted unambiguous identification for nearly two decades. Recently, a picture is emerging[2] which has candidate states at 1.5 GeV and 1.9 GeV.

*An anthropocentric statement, the human eye happens to have three different color sensors.

The main technique is "central hadron production," with the beam and target particles quasielastically scattered and a cluster of hadrons well-separated in momentum space (or more correctly, rapidity, defined in Sec. 2.1) in the center. At high enough energies, this is dominated by double Pomeron exchange, discussed in Sec. 11.2.2.

A proton, observed with a probe with wavelength $\lambda < 0.1$ fm, or $Q^2 > 5$ GeV^2, therefore consists of three valence (constituent) quarks uud, an indefinite number of gluons g which carry about half the total momentum of the proton, and an indefinite number of $q_s\bar{q}_s$ pairs called the sea (s stands for sea). The momentum fraction carried by a parton is called Bjorken-x, or usually just x. Most of the sea quarks are u and d, while strange s-quarks make up about 20% of the total, and charmed quarks, because of their relatively high mass, are present at a lower level. The ratio of c/s quarks depends on Q^2, tending more towards equality at high Q^2, and on x, being predicted to rise from about 0.4 at $x = 0.1$ to 0.8 at $x = 10^{-4}$. At very high Q^2 and very small x, we can expect quark democracy! Even sea top quarks can become nonnegligible at the Very Large Hadron Collider (VLHC, up to 100 TeV/beam).[3]

Phenomenologically, we can consider two hadrons colliding at high energy (such as at the Tevatron, with 900 GeV p and $\bar{p}$ giving a center-of-mass energy $\sqrt{s} = 1800$ GeV) to be colliding broad-band beams of quarks, antiquarks, and gluons. Figure 1 shows a model for a collision involving a hard process.

The spectra of quarks and gluons are dependent, because of evolution, on the Q^2 of the interactions that take place between them. To first (leading) order, these are $2 \to 2$ "elastic" scattering processes: $q\bar{q} \to q\bar{q}$, $q\bar{q} \to gg$, $gg \to q\bar{q}$, and $gg \to gg$. Given that QCD *is* the theory of quark and gluon interactions, we could expect that hadron-hadron collisions are ideal for testing the theory. While hadron-hadron collisions provide a very fertile hunting ground for QCD phenomena (as I hope to convince you), e^+e^- collisions and ep collisions are superior in some respects,[4,5] such as measuring α_S from many features of the final state in e^+e^-. However, quark and gluon scattering processes can only be studied in hadron-hadron collisions, and this is central to QCD.

The scattered quarks and gluons do not emerge from the collisions farther than about 10^{-13} cm, the so-called confinement radius. They have color charge, and as they try to escape, a strong color field builds up in their wake. Unlike the force between two electric charges, which decreases like $1/R^2$, the force between

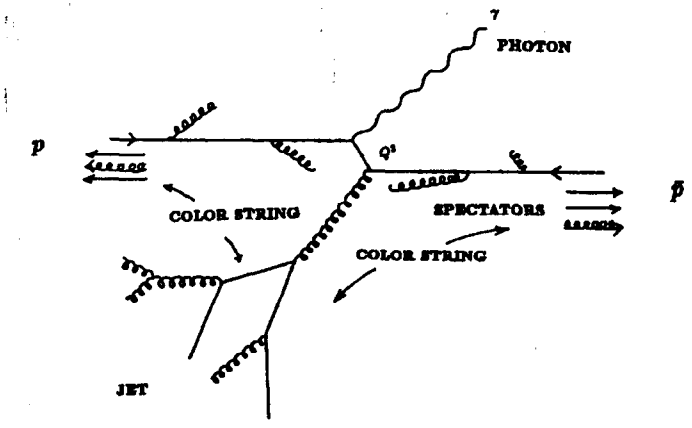

Figure 1: Schematic representation of a hard hadron-hadron collision, as described in the text. A photon is produced opposite a jet.

two color charges remains approximately constant (the potential is linear) with separation, and so the energy in the string-like field increases. (String-like, because if we think in terms of lines of force, these lines behave as if they attract each other, unlike lines of force in QED which behave as if they repel each other.) When the energy in this stretching color field increases, it becomes energetically favorable for a $q\bar{q}$ pair to "pop out" of the vacuum, to be created. This process repeats itself until many quarks and antiquarks with small relative energies, able to form hadrons ... perhaps not yet pions but resonances and low mass colorless clusters ... dominate. The process is called *fragmentation*. In the next stage, the resonances and clusters decay to ground state hadrons, namely $\pi, K, p, \bar{p}, \Lambda$, etc. The above description is a simplified "string model"; the color field is seen as a string which can break, and q and $\bar{q}$ are the ends of the string.

Another picture of fragmentation sees it rather as a branching process, a *tree diagram*. A gluon branches into a quark-antiquark pair $q\bar{q}$ or two gluons gg, a quark branches into qg. At each vertex, a price $\alpha_S(Q^2)$ must be paid in the amplitude, but as the tree evolves Q^2 decreases, α_S increases, and the branching becomes more prolific. Eventually, all these partons assemble themselves into hadrons, and colorless clusters which decay into hadrons, and the proliferation ceases. This is similar in many ways to the string model, and both seem to

be quite good approximations to reality. (Of course, *every* model is at best an approximation to reality.[6])

1.1 Structure Functions

The structure functions or Parton Distribution Functions, PDF's, give the probabilities of finding a quark q_i of type i or a gluon g carrying a momentum fraction x of the hadron, when it is probed with four-momentum-transfer-squared Q^2. Perturbative QCD cannot predict the absolute normalization of parton distributions. However, if given (for example, from a measurement) the distributions at one value of the scale Q^2, QCD *can* calculate them at any other value, provided that both Q^2 are large enough that $\alpha_S(Q^2)$ is small. The name of the game is therefore to choose some *input* PDF, normally at low Q^2, and *evolve* it to larger Q^2 applying the QCD rules of evolution which involve the branching processes $q \to qg, g \to gg$, and $g \to q\bar{q}$.† After the pioneers of evolution calculations Dokshitzer, Gribov, Lipatov, Altarelli, and Parisi,[7] this is called the DGLAP equation. As the evolution occurs, the valence quarks (on average) take lower fractional momentum x, so that the probability of finding a valence quark at high x decreases with Q^2 while the probability of finding one at low x increases. Near $x = 0.2$, the losses and gains cancel out and the quark structure functions are almost independent of Q^2. Dependence only on x, not on Q^2, was a prediction of the parton model and was observed[8] in the Deep Inelastic electron Scattering (DIS) experiments at SLAC in 1969 that gave the first real experimental evidence for the partonic structure of nucleons. However, this observation of DIS scaling was mostly in the region around $x = 0.2$ and was therefore somewhat fortuitous; at both larger and smaller x, the scaling deviations expected in QCD evolution were seen (and were later mapped out) at SLAC.

Unfortunately, we do not have just one arbitrary input structure function, we have one for each quark type $u, \bar{u}, d, \bar{d}, s, \bar{s}$ if we ignore the charm, beauty, and top quarks (which we are normally allowed to do) and one for the gluons g. It is not common, especially in hadron-hadron collisions, to do experiments sensitive to quark helicities, but in principle different helicities can have different structure functions. I shall ignore that complication, but that still leaves seven unknown input functions, which are parameterized with functions typically of the form $q(x) = Ax^B(1-x)^C(1+Dx)$. Usually, the three antiquarks $\bar{u}, \bar{d}$, and $\bar{s}$ are taken to have the same x-dependence and differ only in their normalization, and $s(x) = \bar{s}(x)$. While the u and d quark distributions may be equated with a sum of valence quarks u_v and d_v and sea quarks, the valence distributions u_v and d_v do not have quite the same shape. This can be demonstrated using the rapidity dependence, in $p\bar{p}$ collisions, of the $W^{\pm}$ (the W is the charged weak boson, mass $M_W = 80.3$ GeV) charge asymmetry. The ratio $R(\frac{e^+}{e^-})$ versus η is closely related to the ratio $R(\frac{u}{d})$ versus x.

Despite arbitrariness in the input structure functions (QCD prides itself on calculating their evolution, not the low-Q^2 starting point), there are other constraints. Some of these are sum rules, e.g., because a proton has two u_v and one d_v valence quarks, we must have:

$$\int_0^1 u_v(x)dx = 2 \tag{1}$$

and

$$\int_0^1 d_v(x)dx = 1. \tag{2}$$

There is also a momentum sum rule, integrating over all parton types:

$$\int_0^1 [xq(x) + x\bar{q}(x) + xg(x)]dx = 1. \tag{3}$$

There are also relationships with the phenomenology of Regge exchanges,[45] applied, e.g., to elastic $\gamma^* p$ scattering which involves both *Pomeron* (vacuum quantum number exchange) and *Reggeon* (virtual ρ, f^0, A_2, etc., exchanges). These relations lead one[45] to expect, as $x \to 1$, a behavior $q_v(x) \sim (1-x)^3$. Given the paucity of data for $x \geq 0.75$, this is not contradicted by data. Regge phenomenology also predicts the behavior of the structure functions at the other extreme $x \to 0$ which is now being studied most intensively at HERA.[5] I shall argue that building bridges between QCD (**The** Theory of Strong Interactions, but with limited applicability!) and Regge Theory (which organized a wealth of strong interaction data, mostly outside the domain of applicability—or calculability—of QCD) is now an important and exciting task.

So, the parameterizations of the input structure functions can be (and usually are) constrained by sum rules and perhaps Regge behavior. It is also possible

†Think about the similarities and differences between these branchings in the parton structure of hadrons (hadron→parton) and the branchings in the process parton→hadron described in the previous section. There is a "parton-hadron duality" here.

to say, as Glück, Reya, and Vogt (GRV) did,[9] "What if we just suppose three valence quarks at very low Q^2, sharing the momentum democratically, and let that evolve?" They tried this starting at $Q^2 = 0.5$ GeV^2, but it does not work well . . . of course, using QCD evolution from such low Q^2 is brave. However, if they allow some 50% of the low-Q^2 momentum to be carried by gluons and then evolve, the resulting structure functions are quite reasonable considering the small amount of input. Figure 2 shows the evolved GRV structure functions at very low Q^2 (0.23–0.34 GeV^2) using two evolution procedures, LO and NLO. The Leading Order (LO) calculations compute all the tree diagrams, the branching processes, but do not try to compute diagrams with closed loops. The Next-to-Leading Order (NLO) calculations do allow one-loop diagrams (and must effectively integrate over all possible momenta running inside the loop). The difference between the LO and NLO curves is an indicator that QCD is not a theory with the precision predictive power of QED, basically because $\alpha_S \gg \alpha_{em}$. Allowing two loops (NNLO) and looking for convergence is an obvious progression but is a major piece of work.

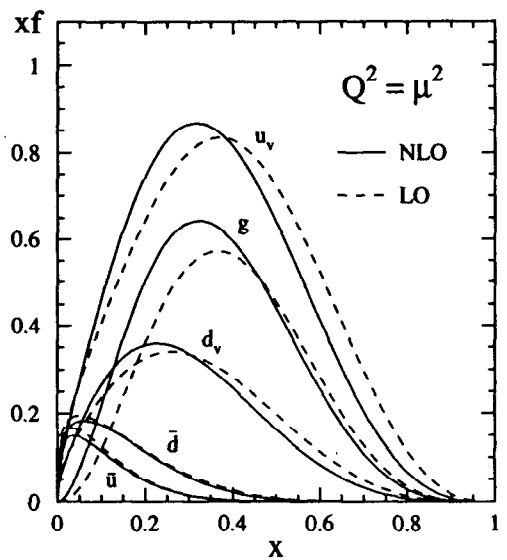

Figure 2: Proton structure functions according to Glück, Reya, and Vogt, at low Q^2.

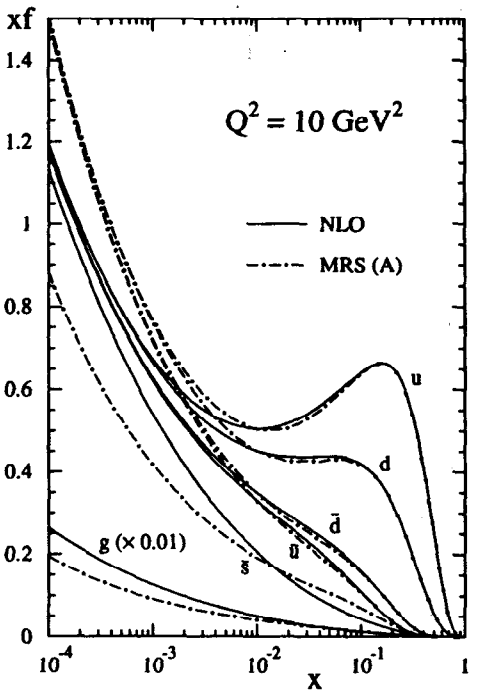

Figure 3: Proton structure functions according to Glück, Reya, and Vogt, on a logarithmic x-scale to show the low-x region.

To see the behavior of the proton structure function at very small x, Fig. 3 shows a plot on a logarithmic x-scale, at $Q^2 = 10$ GeV^2. The antiquarks rise steeply as x decreases from 10^{-2} to 10^{-4}, meeting the quarks as there are no valence quarks here, only sea. The GRV curves show a different trend from an extrapolation of the MRS (Martin, Roberts, and Stirling)[10] fits; there is now HERA data in this region (not available when this plot was made). It is important to be aware that the $xg(x)$ gluon distribution has been scaled down by a factor 0.01 to be shown on this plot! Gluons dominate at small x, by a factor more than three (over the sum of all q and $\bar{q}$ species) at $x = 10^{-4}$. What will happen at still smaller x? When x gets very small, the center of momentum (CM) collision energy of the $\gamma^* p$ collision becomes large; in fact, there is a direct relation between the

low-x structure function and the $\gamma^* p$ total cross section at high energy. In Regge Theory, the total cross section $\sigma_T(s)$ at high energy is determined by the value of the Pomeron trajectory $\alpha(t)$ at $t = 0$. $\alpha(t)$ is the (complex) angular momentum exchanged, and $\sigma_T(s) \sim s^{\alpha(0)-1}$. For the Pomeron $\alpha(0) \approx 1.08$, above 1.0, so $\sigma_T(s)$ increases with (CM energy)^2, s. There is a bound called the Froissart Bound which limits the rise of total cross sections to $ln^2 s$; if they would rise faster, unitarity (the principle that there is no free lunch) would be violated. The interesting question is now "What will happen to $xg(x)$ and $xq(x)$ so that unitarity is not violated as x gets smaller?" Presumably, a flattening or turnover will come in, and will there then be interesting new associated phenomena? Presumably, when this begins to happen, the gluon densities are so high that recombination $gg \to g$ becomes important and cancels the DGLAP branchings $g \to gg$. One also talks about *screening* of color fields becoming important. It is not unreasonable to suppose that this is a frontier (very low x, very high g-density) where new interesting phenomena will show up.

I should not leave this section without referring to "modern" structure function representations which are popular for comparing with hadron collider data. One frequently used set comes from the Martin-Roberts-Stirling (MRS) group in the UK.[10] In addition, a collaboration of theorists and experimenters was formed in the early 1990s, called the CTEQ Collaboration. One of its aims was to provide best-fit QCD-based structure functions to as large a database as possible. These structure functions are labelled CTEQ2M, CTEQ2ML, and so on; Ref. 11 is a useful guide.

2 Quark and Gluon Scattering Processes

We have seen how hadrons can be viewed as microbeams of quarks, antiquarks, and gluons with Q^2-dependent momentum spectra. These partons are continually interacting, but in a frame where the hadron momenta are very large (ideally, the "infinite momentum frame"), due to time dilation these interactions become negligible and we can think of the partons as quasi-independent. When two hadrons collide, a parton carrying momentum fraction x_1 from one hadron can scatter with a parton carrying momentum fraction x_2 from the other hadron. It is usually simplest to think in the center-of-momentum frame, the normal frame of colliders, so that if $x_1 = x_2$, we are also in the parton-parton CM frame. In the center-of-momentum frame, the parton collision energy squared $\hat{s} = x_1 x_2 s = (p_1 + p_2)^2$, where p_i is the four momentum of the parton i in the process $1 + 2 \to 3 + 4$. We also have the four-momentum transfer squared variable $\hat{t} = (p_1 - p_3)^2$ and the crossed variable $\hat{u} = (p_1 - p_4)^2$. For massless partons, $\hat{s} + \hat{t} + \hat{u} = 0$.

There is a simple basic equation for parton-parton scattering in QCD, which is as follows:

$$\frac{d\sigma}{d\hat{t}} = \frac{\pi \alpha_S^2}{\hat{s}^2} |\mathcal{M}|^2. \tag{4}$$

In this equation, $d\sigma$ [cm^2] is an elemental cross section, which if you multiply by the *luminosity* gives the rate of scattering into an elemental $\hat{t}$ bin of size $d\hat{t}$. On the right-hand side, the strong coupling α_S is not a constant (let us **not** call it the strong coupling constant!) but gets smaller as the hardness of the collision Q^2 increases, $\alpha_S(Q^2)$, the so-called running of the strong coupling. What is Q^2 in terms of the Mandelstam variables $\hat{s}, \hat{t}, \hat{u}$? In DIS, it is rather clear that it should be identified with the four-momentum transfer squared of the probing photon/W/Z. Here it is not so clear. $Q^2 = \hat{s}$ would be bad as we can have very soft but very large $\hat{s}$ collisions. On the other hand, for high mass Drell-Yan, $q + \bar{q} \to \mu^+ \mu^-$, $Q^2 = \hat{s}$ would be natural, as the hard photon is in the $\hat{s}$-channel. Choosing $\hat{t}$ is probably good, but should we not have $\hat{t}\hat{u}$ symmetry? The choice

$$Q^2 = \frac{\hat{s}\hat{t}\hat{u}}{\hat{s}^2 + \hat{t}^2 + \hat{u}^2} \tag{5}$$

gives that, and is sometimes used. There is not a unique answer; in fact, theoretically it should not matter which choice is made if one could do the calculations to all orders. The predictions would then be independent of the choice of Q^2 scale. As we are not in that situation, we make a choice, but one that is hopefully not very dependent on the number of orders calculated. One often-used solution is to identify Q^2 with p_T^2 or $(2p_T)^2$ where p_T is the largest p_T object (hadron jet, e.g.) in the event. Given that collider experiments are all central and would not see high mass Drell-Yan giving low-p_T leptons, this should be all right!

There are two other elements of our basic scattering equation: $|\mathcal{M}|^2$ and $\hat{s}^2$, where $|\mathcal{M}|^2$ is a dimensionless number, process dependent, the matrix element for each particular process. From the dimensions of the l.h.s., we can see that the r.h.s. has to have dimensions [GeV^{-4}] as given by the $\hat{s}^2$ in the denominator.

The matrix elements $|\mathcal{M}|$ can be calculated[12] from the Feynman rules for quark and gluon propagators and vertices in QCD, but that would take more theoretical

lectures to explain. Here I will just show the end results for three sample cases. They depend on the quark spins ($\pm\frac{1}{2}$) and colors (3) and gluon spins (-1, 0, +1) and colors (8). These can just be averaged over (initial state) and summed over (final state) if we are not doing spin (color!)-dependent measurements. To give you an idea of what the matrix elements look like, for the elastic scattering of identical type quarks $q_iq_i \to q_iq_i$:

$$|\mathcal{M}|^2 = \frac{4}{9}\left(\frac{\hat{s}^2+\hat{u}^2}{\hat{t}^2}\frac{\hat{s}^2+\hat{t}^2}{\hat{u}^2}\right) - \frac{8}{27}\frac{\hat{s}^2}{\hat{t}\hat{u}}. \tag{6}$$

The annihilation of same-flavor quarks by an $\hat{s}$-channel gluon into a pair of different flavor, $q_i\bar{q}_i \to q_j\bar{q}_j$ is simpler:

$$|\mathcal{M}|^2 = \frac{4}{9}\frac{\hat{t}^2+\hat{u}^2}{\hat{s}^2}, \tag{7}$$

and as a final example, gluon elastic scattering $gg \to gg$ through the four-gluon coupling or $\hat{s}, \hat{t}$, or $\hat{u}$ channel gluon exchange is

$$|\mathcal{M}|^2 = \frac{9}{2}\left(3 - \frac{\hat{u}\hat{t}}{\hat{s}^2} - \frac{\hat{u}\hat{s}}{\hat{t}^2} - \frac{\hat{s}\hat{t}}{\hat{u}^2}\right), \tag{8}$$

and there are similar formulae for several other $2 \to 2$ quark and gluon scattering processes in leading order.

2.1 Rapidity

Rapidity is an important variable and should therefore be defined. Longitudinal rapidity y is just the particle's velocity component along the beam axis, but transformed in such a way that while for small values it is identical to the usual speed $\beta \cdot c = \frac{dz}{dt}$, at large values it does not "saturate" ($\beta \to 1.000\dot{0}$) but keeps going: as $\beta \to 1.000\dot{0}, y \to \infty$. The law of addition of speeds, $\beta_{13} = \beta_{12}+\beta_{23}$ which is only valid at small β, is valid for all values of rapidity: $y_{13} = y_{12} + y_{23}$. So rapidity differences are invariant under Lorentz boosts, and a pion and a proton with the same rapidity are moving with zero relative speed, but have different momenta. We could use a three-dimensional rapidity, and this would be natural in a three-dimensional relativistic world. But generally in particle collisions, one axis has special significance: in hadron-hadron it is the beam-beam axis z and in e^+e^- it is the dijet axis (or thrust axis, defined later). So we choose that as the axis to define a one-dimensional (longitudinal) rapidity, and measure transverse momenta p_T, and transverse energies E_T, with respect to that axis. The linear addition law comes from the following.

From elementary relativity, we have the law for addition of speeds:

$$\beta_{13} = \frac{\beta_{12}+\beta_{23}}{1+\beta_{12}\cdot\beta_{23}}.$$

Where else have we seen this formula? It occurs when adding hyperbolic tans!

$$tanh(A+B) = \frac{tanhA + tanhB}{1 + tanhA \cdot tanhB}.$$

So we just make the identification:

$$\beta_{12} \equiv tanhA,$$

i.e.,

$$tanh^{-1}\beta_{12} = A.$$

This formula has a unique solution:

$$A = \frac{1}{2}ln\frac{1+\beta}{1-\beta}$$

which, as $\beta = p/E$, can be rewritten:

$$y = \frac{1}{2}ln\frac{E+p}{E-p}.$$

A particle of mass m traveling along the rapidity axis with a momentum p has a rapidity $y = ln\frac{E+p_L}{m}$ which is 7.5 for a proton in a 900 + 900 GeV collision. The full rapidity coverage is $\Delta y = ln\frac{s}{m^2}$. If you set $m = 0$ in the above formula for y, you can derive a special case:

$$y_{m=0} \equiv \eta = ln(tan\frac{\theta}{2}).$$

This is called the *pseudorapidity* η and is a good approximation to y as long as the mass m is small compared to p_T. This is perfect for photons but is bad for high E_T jets; never mind, we use it for jets too.

Longitudinal rapidity is a very natural variable in describing final states in hadron-hadron collisions. Particles have an average density of about four charged particles per unit of rapidity, and there are short-range rapidity correlations between particles. To describe jet events, we frequently use E_T, η, and ϕ.

2.2 Event Generators

Given that the strong coupling α_S is not very small, 10^{-1} rather than say 10^{-3}, higher order processes with additional vertices and additional gluons must be considered, the NLO or Next-to-Leading Order processes. This is routinely done, but makes life much more complicated than the nice LO formulae displayed above. The Next-to-Next-to Leading Order (NNLO) processes are now being addressed by theorists, and will eventually take us another step in precision in comparing data with theory.

How are comparisons with theory made in this field? Generally, one copes with the very large number of variables using Monte Carlo methods, *event generators* which simulate interactions on a computer. Basically, one tries to generate interactions taking account of everything we know about parton distribution functions (the relation hadrons → partons), scattering processes, initial and final state radiation (gluon bremsstrahlung), and fragmentation (the relation partons → jets → hadrons). These Monte Carlo generated events must then be confronted with a computer model of the experimental detector, with all its cracks, resolution smearing, etc. Then one can compare data with theoretical expectations, and if one finds significant disagreements, one can try variations of the inputs to, e.g., learn that the received wisdom on PDF's should be modified. Of course, any such changes must not result in significant disagreement with other experiments.

Examples of currently popular event generators are called ISAJET, HERWIG, and PYTHIA. These are big programs developed over perhaps 20 years. Being based on QCD, they, of course, have a great deal in common, but there are also many differences in the way they handle some not yet well-understood subprocesses, for example, fragmentation. These event generators actually have several applications. One is to make predictions, already before an accelerator (SSC, LHC) is approved, for the rates and shapes of diverse event types. For example, a 300 GeV Higgs should decay to W^+W^- and ZZ, and these to four high-p_T jets, but there will be many four-jet events from $gg \to gggg$, so can we still find a signal? Then, when we design the big detectors for such a machine, we use a Monte Carlo simulation to help optimize the detector performance for desired goals (e.g., discovering supersymmetry). While designing the detectors, but more realistically much later, one should use these simulations to devise analysis strategies to optimize signal (SUSY, Higgs) to noise (QCD, Electroweak). Once data exist, observed rates must be corrected for acceptance and resolution and perhaps for subtle effects to derive true cross sections. Because this tends to be a multi-dimensional problem, Monte Carlo methods are the appropriate tool. Finally, the event generators, as a Standard Model benchmark, are compared to the data to look for new physics. The process is iterative and any new physics (which may just be a significant change of the PDF's) will become part of a new benchmark. Where generators differ in their predictions, comparison with experiment can shed light on the not-well-known parts of the physics, e.g., the fragmentation.

Without going into details, let us just look over the main steps in PYTHIA as an example. The parton distribution functions $q_i(x,Q^2)$, $\bar{q}_i(x,Q^2)$, and $g(x,Q^2)$ are built in, with a switch to any particular PDF, and in a pp collision, one can select a parton from each proton with suitable weights (corresponding to the PDF's and the parton cross sections). Initial state gluon radiation from the incoming partons, e.g., $P_{q\to qg}(z)$, where z is the momentum fraction of the quark carried by the gluon, will be simulated. Earlier branchings have smaller Q^2—one starts at a cut-off of about $Q^2 = 1$ GeV^2—and the closer to the hard scattering, the larger is the Q^2 of the radiation. Final state radiation goes the other way, the first branches having highest Q^2.

This description of initial state radiation, scattering, and final state radiation is not quantum mechanically correct. To ask whether a particular hard gluon was radiated just before or just after the scatter is the same as asking which slit the photon went through! But we cannot yet do the calculations properly, with quantum mechanics in all its glory, so we approximate.

The incident partons that do not participate in the hard scattering, the *spectators*, are simulated; as they carry color, color strings may form between these forward moving spectator partons and central scattered partons. The hard scattering uses the QCD matrix elements discussed above, in NLO. The final state partons again form a branching tree, until their *virtualities* (basically Q^2 of the branches) is small. Then comes the part we do not really know how to calculate in QCD, to go from partons to hadrons. So we use some phenomenology, to make the transition to hadrons, not just pions but especially resonances, such as rho-mesons $\rho \to \pi\pi$. PYTHIA also includes some subtler effects such as *color coherence*, which tracks the color fields and gives rise to enhancements or depletions in particle density in certain angular regions, and *color strings*.

3 Experimental Interlude

Experimental lectures should at least say a few words about experiments! The accelerator wizards inject and circulate bunches of protons and antiprotons in opposite directions around the ring, four miles around for the Tevatron and 17 miles for the LHC. The bunches collide at set places around the ring, but they are steered apart electrostatically so that they only meet head-on where there are experiments. The Fermilab Tevatron has two experiments, CDF and DØ. There are about 10^{11} p and $\bar{p}$ per bunch, and they are focused down to transverse dimensions of 30 μm, but only about one $p\bar{p}$ collision takes place per bunch crossing: these particles are very small! However, there are so many bunch crossings per second that the overall rate of interactions is very high (*much* higher than in e^+e^- or ep machines). The rate is

$$R_T = L \cdot \sigma_T, \tag{9}$$

where σ_T is the total cross section, about 80 mb = 8×10^{-26} cm^2 and L is the luminosity, of order 10^{32} cm^{-2} sec^{-1}. The product gives a large number of interactions per second to observe, select, and record. Typically, only tens of events per second are recorded so the combination of the detector and its electronics (*triggers*) must do an amazing job in real time of recognizing which are the events of most interest. After about 15 hours, the beams are degraded in density, so they are dumped and fresh beams are injected. The total *integrated* luminosity over a run is given in units of pb^{-1} or events per picobarn (note that an inverse microbarn is much *smaller* than an inverse nanobarn!).

Hadron collider detectors have evolved but not diverged; most of the so-called general purpose detectors look similar in plan to Fig. 4.

I shall just say a few words about each element with emphasis on their roles in QCD. The figure shows a quarter of the detector; imagine rotating it around the beam pipe to make a cylindrical object and then reflecting in the transverse plane at the left. We really want to detect and identify everything that could come out of a collision: hadrons and leptons (electrons e, muons μ, taus τ, and neutrinos ν), and measure their energies and directions. Starting from the collision point inside the vacuum pipe, the first detector is a *microtracker*, in CDF called a Silicon Vertex Detector. This measures charged particle tracks with very high precision so that one can see the vertices of B-hadron (containing b-quarks) decays displaced from the collision point (although the displacement is only of order

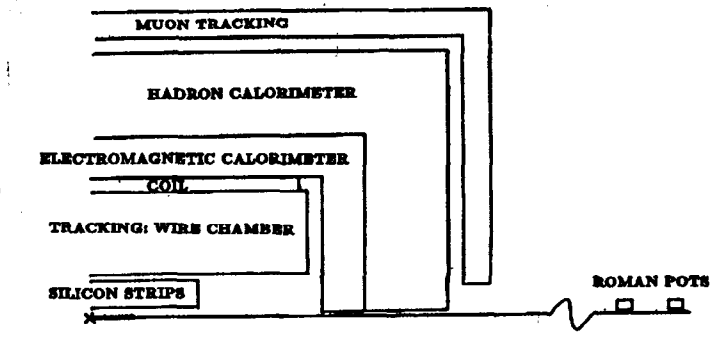

Figure 4: Schematic diagram of a general-purpose hadron collider detector.

of 1 mm). Then the particles pass through a larger tracking volume of lower precision, the whole tracking region being in a magnetic field so the momenta of charged particles can be obtained from their track curvature. The particles then enter two calorimeters; absorbing material that will cause them to shower and deposit all their energy, containing every cm or so a detector layer (liquid argon in DØ and scintillator in CDF, other media are possible). These calorimeters are the heart of the detector for most QCD studies, as they measure the energies of neutral as well as charged particles, and you can see jets (see next section) rather directly in their energy content versus angle. The front part is a separately read out "electromagnetic calorimeter" which detects photons and electrons (a track and shower with $p = E$). This is followed by a thicker "hadronic" calorimeter that contains showers from $\pi^{\pm}, K^{\pm}, K^0_L, p, n$, etc. Not all particles get absorbed in the calorimeters. Muons deposit a few GeV but normally emerge where they can be tracked. Neutrinos emerge (there's not much one can do about that!) but they carry away energy, and in the transverse plane, that can often be detected as missing E_T. If there is more than one large E_T neutrino, only their sum can be measured, but in single W production, the ν can usually be measured quite well by adding the energies vectorially in the whole calorimeter to find the missing E_T.

Way off to the right are two small detectors labeled *Roman Pots*. These are often added to large detectors to detect very small angle and high momentum scattered protons, for studying *diffraction*. This will be discused in Chap. 11.

4 High E_T Jets in Hadron-Hadron Collisions

The first hadron collider was the ISR, Intersecting Storage Rings, at CERN. The first collisions took place in 1971, just 25 years ago, in the same year that an important paper was published by Berman, Bjorken, and Kogut[13] (BBK) predicting high p_T jets in hadron collisions. At that time, the highest energy (fixed target) pp collisions were at 30 GeV beam energy, i.e., 7.6 GeV in the center of mass. The ISR was to take us to 63 GeV in the CM, equivalent to 2000 GeV with a beam + fixed target. The conventional wisdom then was that in hadron-hadron collisions, particles are produced with limited p_T, with a typical distribution e^{-6p_T}. The chance of finding a particle with p_T as high as 5 GeV/c from such a distribution is rather small! The main "facility" magnet, called the Split Field Magnet (SFM), was chosen to have a good field only in the forward (beam) directions, because "that is where all the physics would be," and a proposal for a central axial field magnet was not approved. The BBK paper pointed out that in the then-new parton model, which was looking good because the SLAC experiments[8] seemed to be seeing charged partons by the electromagnetic interaction, we should also have strong interaction scattering between the partons. Strong $qq \to qq$ scattering (assuming partons are quarks) was not yet calculable (this was pre-QCD), but BBK estimated that the strong scattering could be as much as 10^4 times stronger than electromagnetic (an overestimate because BBK did not know $\alpha_S \approx 0.1$). So what would events look like if two partons made a large angle scatter? BBK said the partons would turn into jets of hadrons! (They actually used the word "cores.") They were absolutely right, and although this paper inspired high p_T jet searches at the ISR, the wheels turned painfully slowly. An abundance of hadrons, both π^0 and identified charged hadrons π, K, p, and $\bar{p}$ at large p_T (of order 4–10 GeV), was discovered, and eventually only the hard parton scattering explanation survived. At Fermilab with its lower energy ($\sqrt{s}$ = 24 GeV) fixed-target collisions, one looked[14] for jets by triggering on total transverse energy E_T in limited solid angle calorimeters, but this had a very strong bias making the results difficult to interpret. It was agreed that the trigger solid angle must be much larger than the eventual jet solid angle, so that the jets are much more localized than had been required in the trigger. It was finally 11 years after the BBK paper, in 1982, that really convincing evidence for high p_T jets was presented from the ISR,[15] made possible by a really good (uranium-scintillator) large aperture hadron calorimeter and very high luminosity from the machine. An example is shown in Fig. 5, an early example of a so-called LEGO plot.[16]

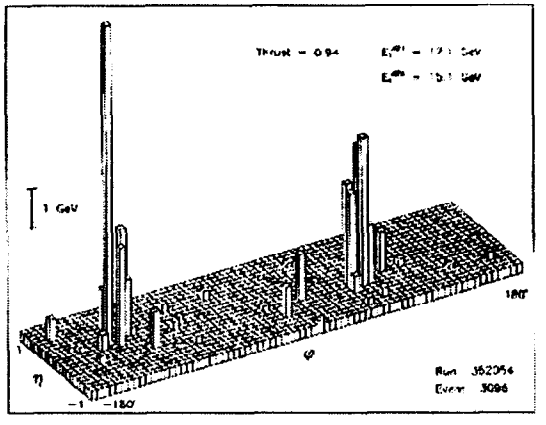

Figure 5: A high E_T jet event at the ISR. The E_T detected in cells in η and ϕ is shown; the trigger/selection was just large total E_T.

Each calorimeter cell (tower) is shown as a cell in the $\eta\phi$ plane with a vertical bar proportional to the $E_T = E \cdot sin\theta$ in the tower. On the figure, the quantity Thrust = 0.94 is noted. Thrust, T, is a quantity defined as:

$$T = Max\left(\frac{\sum|\hat{e}.\vec{p}_i|}{\sum|\vec{p}_i|}\right), \tag{10}$$

where the sums are over all clusters with vector momenta $\vec{p}_i$ in the transverse plane and $\hat{e}$ is a unit vector in the transverse plane. It can range from $2/\pi = 0.64$ for an isotropic event to 1.0 for a perfectly collimated two-jet event. The event in the figure is not atypical once ΣE_T in this central region exceeds about 35 GeV (out of $\sqrt{s}$ = 63 GeV), although this only happens in about one in 10^9 collisions.

By this time, experiments UA1 and UA2 at the CERN $p\bar{p}$ Collider were beginning to present their first results. Even though their luminosity was still very low, thanks to the much higher $\sqrt{s}$ = 540 GeV, events with dramatically high (at that time) p_T jets could be clearly seen.[17,18] So the discovery of high p_T jets in hadron collisions was shared between the ISR and $Sp\bar{p}S$, but the latter was in the limelight and provided a dramatic and exciting first look at the new era of

jet physics. At the new generation of colliders ($Sp\bar{p}S$, Tevatron, LEP, LHC), we would come to treat jets like particles.

In the early days of measuring jets, one much-discussed question was: "What is the best way to define a jet?" and various *jet algorithms* were proposed. A typical and still much used algorithm is to find a cone in $\eta\phi$ space ... actually, it is a *circle* in $\eta\phi$ space which is two-dimensional ... chosen to contain a local maximum in ΣE_T, the total transverse energy of all hadrons, or calorimeter towers, in the circle. This is called a *cone algorithm*; in the central region, the $\eta\phi$ circle corresponds to a good approximation to a circular cone in space, although when it is very forward, the cone gets distorted. Actual procedures are usually iterative, starting with the highest E_T calorimeter cluster and putting a cone around it, adding the "energy vectors" inside to define a new cone axis, and repeating if necessary until some condition is satisfied. Once the procedure is defined, the only parameter to be chosen is the cone radius $R = r_{max}$, where $R^2 = \Delta\eta^2 + \Delta\phi^2$ and $\Delta\eta$ and $\Delta\phi$ are the distances of a particle (or calorimeter tower) to the cone axis. Cone radii are typically chosen in the range 0.4 to 0.7, values which hopefully give an optimum correspondence between the measured jet four-momentum and the "initiating hard parton" (even though the latter is not theoretically well-defined because of Quantum Mechanics). If you make the defining cone too small, particles obviously associated with the hard scatter are excluded, and if it is too large, more of what is often called the *underlying event* is included. The underlying event is also not a well-defined concept; in reality, color connections are everywhere in an event, and it does not make sense to ask whether a pion with $p_T = 600$ MeV/c and $r = 0.8$ is part of the jet or of the "underlying event." The color-string model takes this holistic view. But cone algorithms ideally choose a cone size where (a) leakage of "jet particles" out is on average balanced by an "underlying event" taken in. (b) A hard, perturbatively radiated gluon will be reconstructed as a separate jet and not merged in. Again, there is no sharp cut-off between hard and soft radiation, so finally one must just do the same things with the same cuts in data and Monte Carlo generated events and compare them. For any "reasonable" choice, it should not matter what cone size is chosen. CDF and DØ normally (but not always) use 0.7 independent of E_T. For a multijet process like $t\bar{t} \rightarrow 6$ jets, 0.4 is preferred. As jets tend to shrink in $\eta\phi$ space with E_T, one could make $R(E_T)$, but this complication is not normally worth making. What about the low E_T end, how far down can one go in E_T and still talk meaningfully about jets? This is a complicated question and there is no sharp boundary. It is also a machine-dependent question. In e^+e^- collisions, the first two-jet structures were observed at $\sqrt{s} = 6.2$–7.4 GeV (Ref. 19), but they became much more obvious at higher energies, e.g., when PEP and PETRA operated at $\sqrt{s} = 30$ GeV. These are intrinsically clean final states with a q and $\bar{q}$ back-to-back. In hadron-hadron collisions, it is a different matter, with a large number of final state partons, most going forward-backward (and giving rise to the so-called underlying event). Jets obviously will need higher E_T to stick out of this "background." This statement will also be dependent on $\sqrt{s}$. At the lowest $\sqrt{s}$ hadron collider, the ISR, the AFS Collaboration measured jets down to 6 GeV in fair agreement with hard scattering models, but only by about 10–12 GeV were they the dominant feature in a large solid angle trigger. At the $Sp\bar{p}S$ and Tevatron, it is generally considered that jets above about 10 GeV E_T "make sense," i.e., the measured jet momentum corresponds reasonably well to a hard parton, while jets below about 5 GeV do not, i.e., the correspondence is very washed out. However, a recent CDF study has found that if you select collisions with exactly two "jets," both with $5 \leq E_T \leq 7$ GeV, they will nearly always be back-to-back in azimuth, showing that even at the Tevatron (not just at the ISR) such a low E_T cut can sometimes be used. Where one chooses to cut depends on the physics under study. In events at the Tevatron with $\Sigma E_T > 500$ GeV, jets of 5 GeV are lost, but in double Pomeron events with $\Sigma E_T \sim 20$ GeV, they stick out.

Jet E_T spectra rise dramatically with $\sqrt{s}$. The ISR was put out of business by the $Sp\bar{p}S$, and the $Sp\bar{p}S$ by the Tevatron, and you can see a comparison[20] between the latter two in Fig. 6.

Actually, the data is all from CDF at the Tevatron, but the two lower energies were chosen to coincide with the $Sp\bar{p}S$. At $E_T = 100$ GeV, the $\sqrt{s} = 1800$ GeV (Tevatron) jet production cross section is 40 times what it was at $Sp\bar{p}S$. The rise is because at the higher $\sqrt{s}$, the scattering partons are at lower x where the parton density is much higher (and more are gluons, which helps). At 1800 GeV, the data span eight orders of magnitude in rate (using 1/5 of the data to date) and reach above 400 GeV in E_T. On nearly every point, the statistical error bars are smaller than the symbols. Experiment DØ has data that agree extremely well with this 1800 GeV spectrum. What is very impressive is the agreement with a typical theoretical calculation as shown by the lines. Only at the largest E_T, above say 250 GeV, does a disagreement appear at the level of a factor of about 1.5.

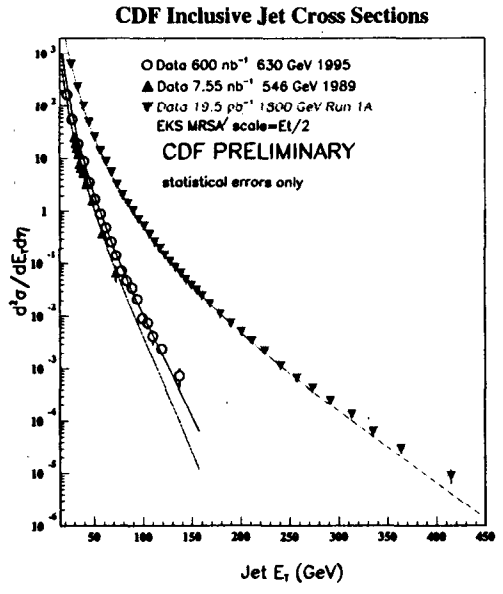

Figure 6: Inclusive jet cross section at three s values, as measured by CDF in the central region. The two lower energies correspond to the $Sp\bar{p}S$.

The disagreement is seen more clearly on a linear scale by dividing data by theory and subtracting 1, or (DATA-THEORY)/THEORY, and this is shown in Fig. 7. The points below 200 GeV are low but if you include systematic errors which are about 20% (largely E_T independent), they agree. The so-called "excess" at high E_T is clearly not a statistical fluctuation, and CDF could not find a systematic (or detector) effect which would account for it. A real excess that could not be explained by QCD would be exciting as these jets are probing quarks (mainly) at smaller distances than ever before, and if quarks were really composite at the scale of order (1.5–2.0 TeV)$^{-1}$ (about 10^{-17} cm), this is the sort of thing one might see. The DØ jet data could not quite either confirm or deny an excess: their high E_T data points were lower than CDF's but not by more than 1–2 σ.

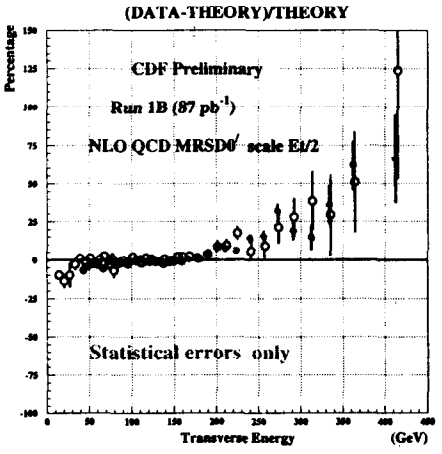

Figure 7: A comparison of the inclusive jet cross section with the NLO QCD calculation using the MRSD0′ structure function.

Before jumping to conclusions about dramatic new physics, one has to see whether some not-so-dramatic new physics can explain the discrepancy. There are two worthy contenders: (1) the density of gluons in the $p/\bar{p}$ at large x is more than in the structure functions being used for comparison (CTEQ3M, MRSD0′, and others) or (2) soft and colinear gluon corrections are important.[24] As to the former possibility, of course, one cannot just try adding in more gluons at high x because that will change all the fits to other data, such as DIS data. A new global fit has to be tried to find a solution consistent with all good data. Normally, the high E_T jet data would have little relative weight in such a fit and would not pull the structure functions. So CTEQ tried a fit giving extra weight to the high E_T data by artificially decreasing their errors, and found a solution CTEQ4HJ, shown in Fig. 8 with both CDF and DØ data. This makes the excess insignificant without significantly worsening the fit to the rest of the world. In their fit, the normalizations of CDF and DØ were left floating, but they only moved 2% which is impressive. So, one simple solution to the excess puzzle is to

modify the structure functions mostly at high x by just about doubling the glue. More data to shed light on this could come from probing the high rapidity tails of the jet distributions at lower E_T.

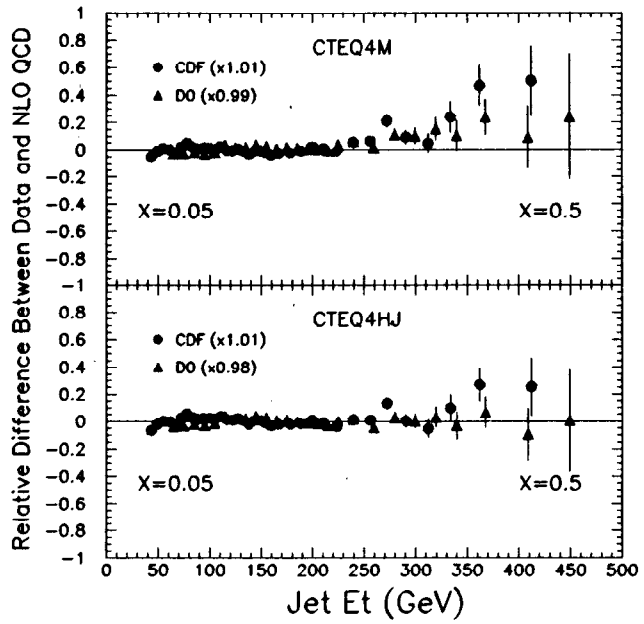

Figure 8: Linearized comparison [(DATA-THEORY)/THEORY] of inclusive jet data.

An alternative, or perhaps additional, way[24] of explaining the jet rate at very large E_T is to consider higher order corrections. While the full NNLO calculations have not been done (and it may be some time!), direct estimates of higher order corrections are sometimes possible by a process called resummation. This generally requires two hard scales in the process with one much larger than the other, say $Q \gg \mu$ where μ is the inverse wavelength of emitted gluons. Soft colinear gluons cannot know about the hard scattering taking place on the much smaller scale $1/Q$. In such cases, it is sometimes possible to resum the large corrections which have the form $\alpha_S \cdot log^k(Q/\mu)$ (resumming large logarithms). See Refs. 22 and 23 for more information. Very high $x_T = 2E_T/\sqrt{s}$ requires partons from very high Bjorken-x where the parton densities are falling fast and the phase space for gluon emission is reduced; this will affect the jet cross sections in the right direction to explain the excess, but according to Mangano,[24] "it seems unlikely that the full 30–50% excess reported by CDF ... could be explained by resummation effects."

The CDF two-jet mass spectrum, shown in Fig. 9, perhaps not surprisingly, shows the same excellent agreement at low mass with a growing excess compared to PYTHIA (CTEQ2L) at large mass. It is to a large extent the same data, so this is not independent. It is still impressive to note that we are now detecting parton collisions at $\sqrt{\hat{s}} = 1000$ GeV, and if there were strongly produced new particles, such as *"axigluons"* up to a mass of 870 GeV, they would be visible in this plot as a significant bump.[25] Several other types of hypothetical massive particles can also be excluded, thanks to our knowledge (or assumed knowledge) of their strong interactions, namely QCD. This search will be continued in the Tevatron Run II (1999–?), but a really large extension of the mass range will only come with the LHC.

Naturally, one of the first questions to ask, faced with a possible large E_T jet excess, is whether the angular (or η) distribution of these jets is normal. It is. To see this for dijets, we can calculate a variable χ defined as:

$$\chi = \frac{1 + cos\theta^*}{1 - cos\theta^*} = |e^{\eta_1 - \eta_2}|. \tag{11}$$

Figure 10 shows some χ distributions together with NLO predictions, and the fit is good for all mass ranges. From this, a lower limit can be put on a parameter Λ_C which is called the *compositeness scale*, namely Λ_C >1.8 TeV at 95% confidence level. Thus at a resolution of about 1.1×10^{-17} cm, the partons still appear point-like.

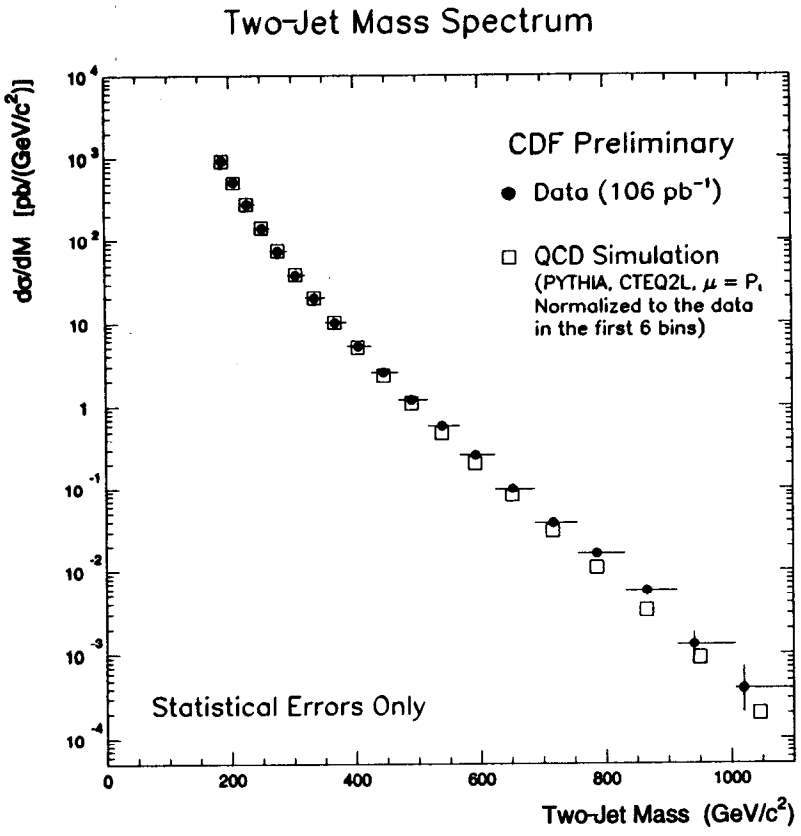

Figure 9: Spectrum of the invariant mass of the two highest jets.

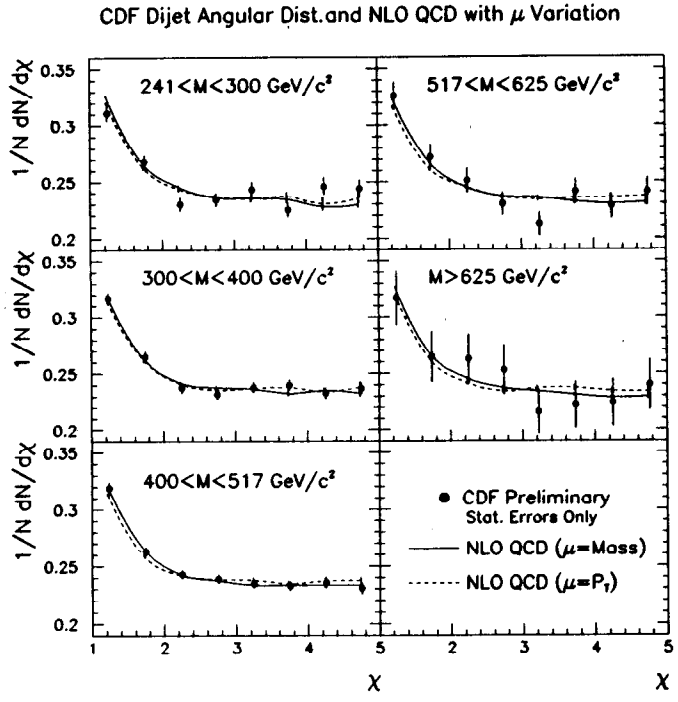

Figure 10: Angular distribution of the two highest jets in terms of the variable χ (see text).

Another place where large logarithms appear is when two balancing jets are at large opposite rapidity, or small angles. Then $log\left(\frac{\hat{s}}{Q^2}\right)$ is large and we can apply resummation schemes. Important progress in this direction came with the BFKL formalism from Balitsky, Fadin, Kuraev, and Lipatov.[26] A picture emerges of gluons scattering by t-channel gluon exchange, the latter also emitting gluons, so that this diagram times its complex conjugate is like a *ladder*. This is a perhaps naïve description of the BFKL Pomeron, not the same as the standard Pomeron giving diffraction with rapidity gaps (about which more will be said later), but related. The BFKL Pomeron is much discussed in relation to very low-x physics. DØ searched[27] for evidence in the form of a decorrelation between a pair of hadron jets as the rapidity interval between the jets increases. Figure 11 shows the azimuth angle difference $(1 - \Delta\phi/\pi)$; the back-to-back peaking has a tendency to wash out as $\Delta\eta$ increases. However, as seen in Fig. 12, the effect is not as strong as predicted by BFKL and is actually in agreement with the HERWIG Monte Carlo (but not NLO JETRAD). BFKL effects are seen elsewhere (e.g., at HERA) and more studies are clearly needed.

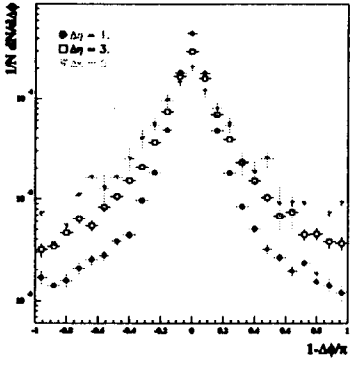

Figure 11: The azimuthal difference between the two leading jets (DØ) for three different values of their rapidity separation. The back-to-back balance gets washed out as $\Delta\eta$ increases.

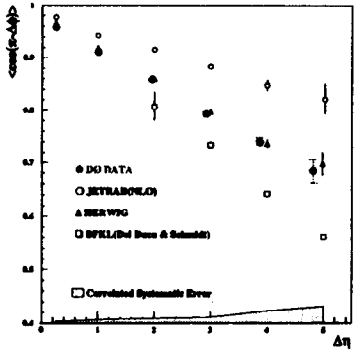

Figure 12: The mean value of $< cos(\pi - \Delta\phi) >$ versus $\Delta\eta$ showing the decorrelation of the previous plot, compared with three predictions.

4.1 Multiple Jets: Very High E_T

In the previous section, I discussed inclusive one-jet and two-jet data, but events with many high E_T jets are not rare at the Tevatron, and they provide an interesting testing ground for the QCD predictions *via* MC. One can study both the total rates and the structure of the events, e.g., sub-energies and angles between jets. Figure 13 shows CDF data, ignoring everything in the events except jets above $E_T = 20$ GeV and making a scalar sum of those above that threshold. The data are only plotted above $\sum E_T = 300$ GeV, far above any threshold effects, and extend to about 1000 GeV. The shape compares well with the two Monte Carlos (JETRAD and HERWIG) apart from being slightly flatter at large E_T, the same effect we saw in the one-jet inclusive spectrum (it is, of course, essentially the same data). The relative normalization of 1.4 applied to the MC to get best agreement is probably as good as could be expected for these far-from-simple events. Still, although the highest $\sum E_T$ events frequently have several jets, the two highest E_T jets usually dominate.

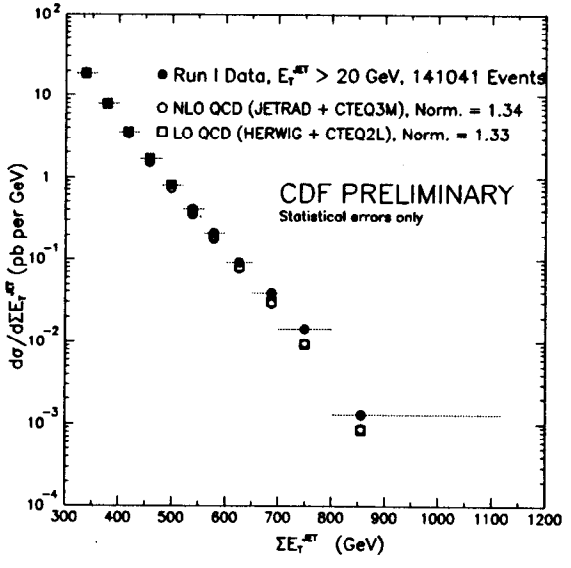

Figure 13: Distributions of total E_T including all jets above 20 GeV.

CDF did a study[21] of events with $\sum E_T$ above 420 GeV and three jets each above 20 GeV. There are many ways to study data with many variables, so one should try to choose plots that have a clear physical meaning, or which make incisive tests among models. Figure 14 (Ref. 21) shows the mass distribution of the three, four, or five highest E_T jets compared with HERWIG and NJETS; both give good descriptions. For three jets, one can go to their rest frame, calculate the energy fraction

$$X_j = \frac{2E_j}{m_{3j}}, \tag{12}$$

and make a Dalitz plot of X_1, X_2, and X_3. This sort of study can also be done for four-jet events by merging the two jets with the smallest invariant mass m_{ij} to get a three-body system (with an additional variable m_{ij}). Any number of jets can be sequentially reduced this way to a three-body system which can then be studied more simply. For example, the distribution of X_3 for three-jet events (all above 20 GeV) seems to be a variable with little discriminating power, both phase space and QCD Monte Carlo having similar behavior and agreeing with data, apart from a wave in HERWIG which the data does not show. Phase space models do not describe the data as well as the QCD calculations which predict large contributions from initial or final state gluon radiation.

5 Direct Photon Production: γ and $\gamma\gamma$

As quarks carry electromagnetic charge as well as strong charge, in any diagram involving gluon emission from a quark $q \to qg$, we can also have photon emission $q \to q\gamma$. The leading order diagrams are $qg \to \gamma q$ and $q\bar{q} \to \gamma g$, and there are also bremsstrahlung photons radiated off quark lines. The latter are usually considered as a background and are harder to measure, being close to (or in) a hadron jet. Therefore, experiments usually require the photon candidates to be *isolated*, to have very little accompanying energy in a cone of $R = 0.4$ (typically). This cut also minimizes background from π^0; most detectors cannot resolve the two photons from $\pi^0 \to \gamma\gamma$ at high p_T, but π^0 tends to be in jets.

Direct photon production at high p_T was first observed at the ISR.[29] As they had done for jets, the $Sp\bar{p}S$ and Tevatron extended the reach in p_T dramatically, up to about 120 GeV in the latter case as shown in Fig. 15. It is not enough to require an isolated electromagnetic shower; the background from π^0 is still high.

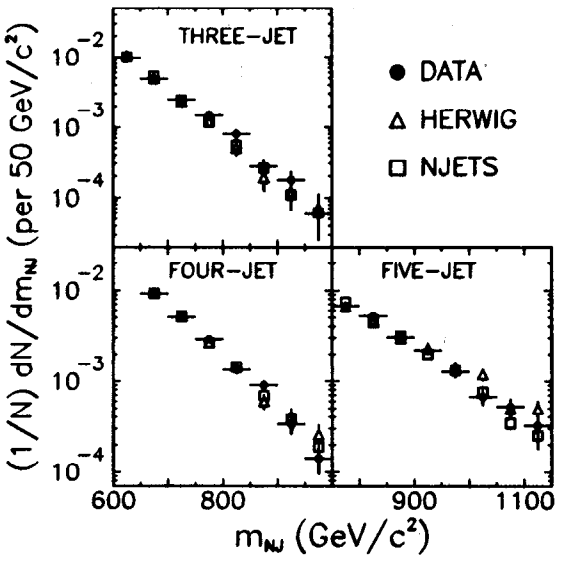

Figure 14: Distributions of the effective masses of the three leading jets, four leading jets, and five leading jets (if present, above 20 GeV). The data are compared with HERWIG and NJETS and agree well.

A method of statistically separating the γ and π^0 pioneered by UA2 (Ref. 30) is to start the calorimeter with a converter and then a separately read-out layer to see whether a photon conversion occurred. The probability for the two photons from a π^0 to convert is about twice the probability for a single direct photon, so it is easy to calculate the fraction of γ in the sample (although not on an event-by-event basis). This method can be used at arbitrarily high p_T. The CDF calorimeter also has a so-called Shower Maximum detector, a layer of strip elements after a few radiation lengths (near the maximum of a typical shower) which can measure the projected profile. The two photons from low energy π^0 are resolved into two peaks (depending on the decay orientation), but even at higher E_T when they merge (typically, in CDF, the shower separation is $d_{\gamma\gamma} = 50$ cm$/E_{\pi^0}$), the profile is broader for π^0. The figure shows that both methods agree where they overlap, and also that the data agree well with NLO QCD, at least at high p_T, with the CTEQ2M structure function. We could expect that photons are better probes of

structure functions than jets; there are none of the complications of final state radiation, jet fragmentation, or questions about the correspondence between the jet and hard parton. Calorimetric detectors also have better resolution for photons than for hadrons, and it is intrinsically a clean process. So it was hoped that the diagram $gq \to q\gamma$ would be a good way to measure the gluon distribution $g(x, Q^2)$. However, higher order diagrams muddy the predictions, and they are not as precise a probe as once thought.

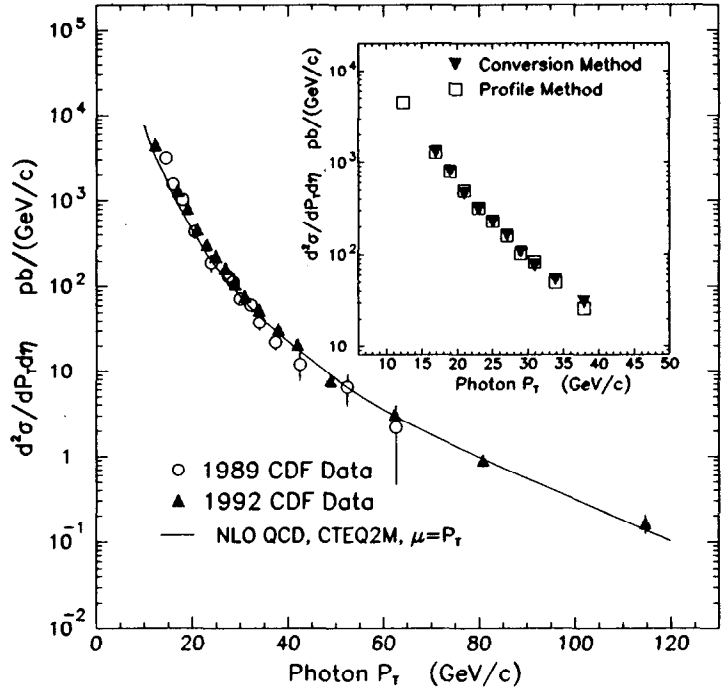

Figure 15: The p_T spectrum of direct photons as measured by CDF, compared to a NLO calculation which underestimates the rate at low p_T. The inset shows the agreement between two methods of identifying photons (conversion probability and shower profile).

In detail, the photon data lie systematically above the QCD line below 40 GeV. *All* direct photon data are systematically high at their lowest p_T values. If this were

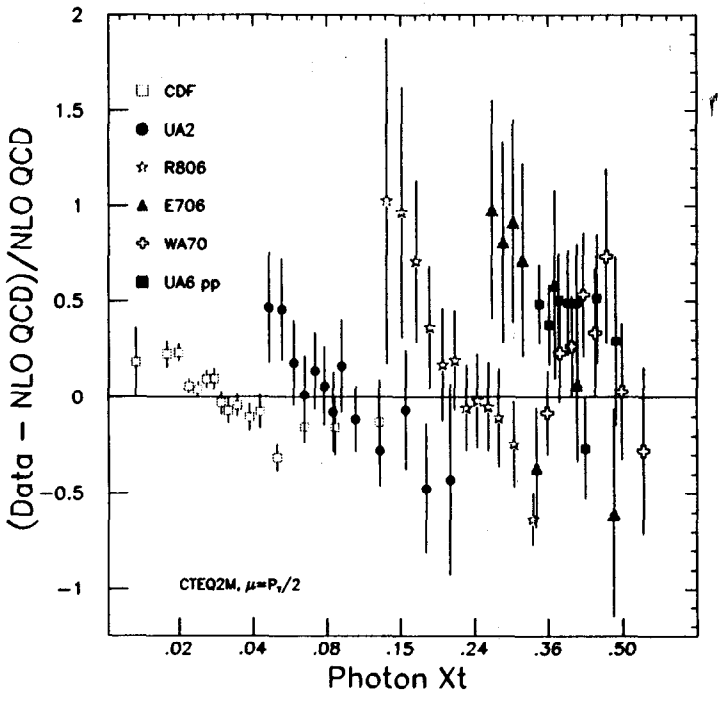

Figure 16: The x_t spectrum of direct photons in different experiments (data-theory/theory). The lowest p_T data are systematically high.

due to a structure function behavior, we would expect the trend to be common, to experiments at different $\sqrt{s}$, if plotted against the scaled p_T, namely, $x_T = 2p_T/\sqrt{s}$. In Fig. 16, (Data-NLOQCD)/NLOQCD are plotted and show that this is not the simple solution; at the same x_T, a low $\sqrt{s}$ point is higher than QCD, and a high $\sqrt{s}$ point is lower. Admittedly, these points differ in Q^2, but the Q^2 dependence is supposed to be well-handled by the QCD calculation. It looks like an effect that to first order is a p_T dependence, the lowest p_T being enhanced at any $\sqrt{s}$. A likely explanation is that the QCD predictions fail because they assume that the incoming partons are colinear. We know that cannot be strictly true because protons have a finite size, so the uncertainty principle will give an *intrinsic* k_T of a few hundred MeV/c to the partons. But more than that, there

are nonperturbative (and therefore not well-calculable) effects, namely, soft gluon emission, that can give k_T which may be larger than a GeV and will smear the production cross section. This k_T (which I would not call intrinsic, I reserve that for the proton size effect) will depend on $\sqrt{s}$ at fixed x and could account for much or perhaps all of the behavior in Fig. 16. But the jury is still out. One good test should be two photon production.

The production of two back-to-back high p_T direct photons was first seen at the ISR,[31] but the signals there were very small. Even at the Tevatron, very few events were found by CDF in 90 pb^{-1} as shown by the plot of $M_{\gamma\gamma}$, Fig. 17. In this plot, the rise to $M_{\gamma\gamma} \approx 30$ GeV is entirely a trigger threshold and data selection effect; presumably the cross section is very high for low mass pairs, all the way down to the GeV region and below, but the experiment has not been done. (It might be very interesting.) Can we conclude anything about k_T from this limited data? The diphoton system p_T is well-measured, but the poor statistics can be seen in Fig. 18. What can you say?

On a separate issue, note that $M_{\gamma\gamma}$ is well-determined by good electromagnetic calorimeters, obviously much better determined than M_{JJ}. For best resolution, one needs to know also the production point, not always easy at a high luminosity hadron collider such as LHC. But this is why the two-photon channel is considered an interesting channel for searching for Higgs H^0 even though the branching fraction of $H \to \gamma\gamma$ is very small, less than 10^{-4} depending on M_H. Between about 80 GeV and 150 GeV (the intermediate mass Higgs region), the full width of the Higgs is only a few MeV, much narrower than conceivable resolutions (so an experiment with super resolution has a major advantage). There is a very interesting thing about this decay which makes it important even if the H^0 is discovered in another channel. The H^0 being neutral does not actually couple to photons, so this decay proceeds through loops of anything that couples both to H^0 and γ, and the heavier the better. This means the decay rate will depend on the existence of heavy things such as W, t, $\tilde{q}$, and even charged particles of many TeV, or even hundreds of TeV. But it will be difficult! Very!

6 Vector Bosons: W/Z + Jets

Just as direct photons can be used as probes of hard QCD processes, so can vector bosons, namely, $W^{\pm}$ and Z. In lowest order, the perturbative diagrams are simply

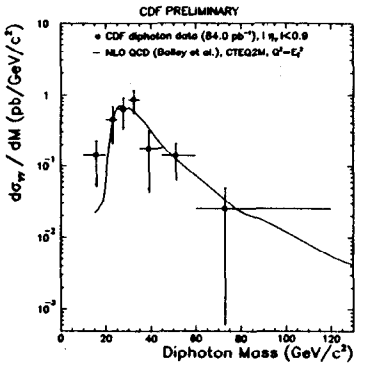

Figure 17: The diphoton mass spectrum measured in CDF. The rise at low $M_{\gamma\gamma}$ is due to threshold/acceptance effects.

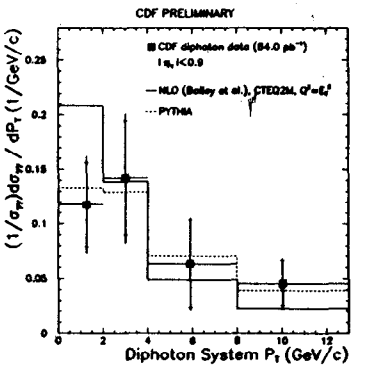

Figure 18: The distribution in p_T of the $\gamma\gamma$ pair. This should be a useful probe of k_T effects.

$q\bar{q}$ annihilation, $q\bar{q} \to W$, and the W have low p_T which is given by, and provides information on, nonperturbative initial state gluon radiation and k_T (I do not now distinguish these). This process is like Drell-Yan ($q\bar{q} \to l^+l^-$) and is sometimes also called Drell-Yan. Given that a colored quark from the proton annihilates with a colored antiquark, with a large rapidity separation, perhaps the associated hadrons in these events would show interesting differences with, e.g., typical soft collisions. To the extent that people have looked (which does not include the forward regions), there are no striking differences.

More study has been done of events containing both a W/Z and high p_T jets. Apart from the intrinsic interest for QCD, $W + jets$ is the most important channel for studying the top quark. The dominant process for creating top quarks is $q\bar{q} \to t\bar{t}$ and then $t\bar{t} \to W^+bW^-\bar{b}$. The W then decay either hadronically $W \to q\bar{q}$ or leptonically $W \to l\nu$. If both W decay hadronically, which happens 46% of the time, we have a six jet final state. Strong QCD production of six jets has a much higher cross section, but a $t\bar{t}$ signal can still be observed[32] by demanding that one or two of the jets have characteristics of b jets (leptons from semileptonic b decay, or displaced vertices). When both W decay leptonically (10% of the time for each of e, μ, or τ for each W), the signature is relatively clean, but two neutrinos are undetected so the kinematics is poorly constrained. The best compromise between

signal:background and reconstruction ability is with the 44% fraction which are hadronic+leptonic, called the *lepton + jets* mode. There is still a large background from non-top W + jets, hence the importance of being sure we understand the QCD aspects. Note, however, that two of the jets in $t\bar{t}$ production will be b-jets, so b-tagging is very important. Unfortunately, b-tagging efficiencies are typically only about 30%–40%.

The cross section for $W + \geq n$ jets and $Z + \geq n$ jets[33] as functions of the number (actually $\geq n$) of jets is shown in Fig. 19. Jets are counted if their E_T exceeds 15 GeV and they are in the pseudorapidity region $|\eta| \leq 2.4$. Note the excellent fit to a pure exponential, with a factor of five decrease for each additional jet. This factor will depend on the minimum jet E_T. Note also that the Z cross sections are just about a factor of ten below the W (mostly because of the mass difference), and show the same behavior. Leading order QCD predictions using VECBOS and MRSA and CTEQ3M structure functions and two different choices of Q^2 are also shown, giving some idea of the uncertainty coming from the choice of renormalization scale. The cross section for W + 4 jets (with the above cuts) is about 5 pb^{-1}. Compare this with the cross section for $t\bar{t}$ [$7.7^{+1.8}_{-1.5}$ pb from CDF, and 5.8 ± 1.8 pb from DØ (for $M_t = 170$ GeV)] times the 0.43 combined branching fraction. I do not go into additional complications in the top studies such as: one or more of the wanted jets from top decays may be below threshold or at too large η, and additional jets from gluon radiation may be in the selected region. These effects are all supposed to be modeled correctly in the Monte Carlo simulations.

There are many measurements one can make and compare with perturbative QCD in W/Z + multijets events. I will just show one and mention a few more. Figure 20 shows the E_T of the highest E_T jet associated with a W. There are a few events with a jet above 150 GeV.

The spectrum includes the estimated contribution from $t\bar{t}$ events *(background!)*, from jets from other interactions (pile-up), and "QCD background" which means that a hadron jet fakes a W. The sum of all these fits the data reasonably well, but the data above 120 GeV are systematically high. Other plots agree remarkably well; these include:

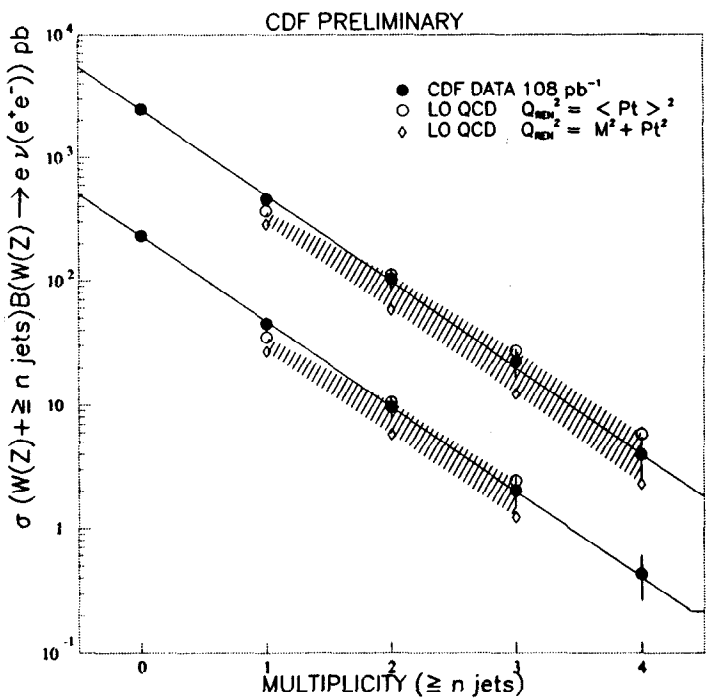

Figure 19: The multiplicity of jets in events with a W (top curve) and Z (bottom curve). The lines are simply exponential fits. The shaded band shows LO QCD and the effect of varying Q^2 within the range shown.

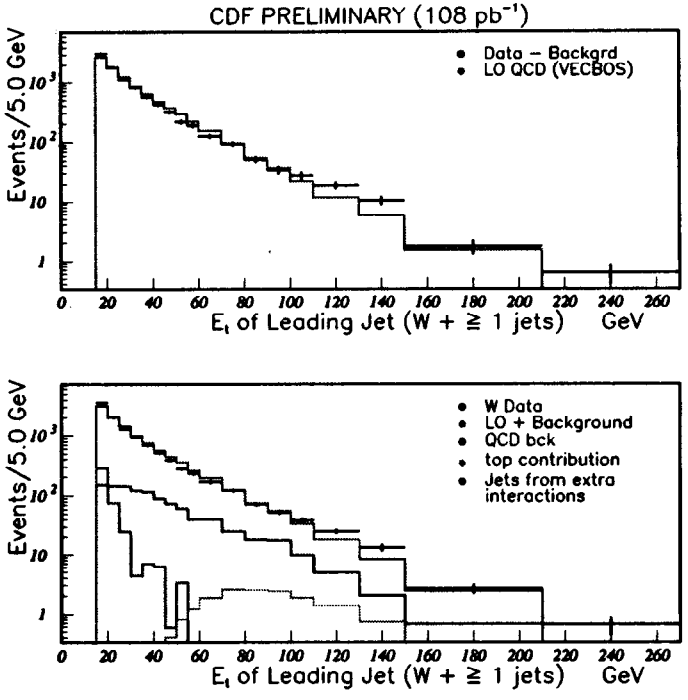

Figure 20: In a study of jets associated with W, the top plot shows the E_T spectrum of the leading jet and the bottom plot shows the predictions for how this is composed.

- The E_T distributions of jets two and three if present.
- The dijet mass distributions if two or more jets are present. It extends to about 650 GeV. There is no sign of any extra events in the W/Z region from WW or WZ production!
- The distance ΔR_{ij} in the $\eta\phi$ plane between two jets.
- $E_{T2} + E_{T3}$ . . . and so on.

7 Heavy Quark Production: Charm, Beauty, and Top

In this section, we consider c, b, and t quark production; these are normally considered the heavy quarks. The production of strange s quarks, including $\phi(s\bar{s})$ mesons, cannot be calculated in perturbative QCD. Such small mass means too large α_S to handle. For top ($M_t \approx 175$ GeV) and bottom ($M_b \approx 4.1$–4.5 GeV), perturbative QCD should work rather well, and we can test that. The charm quark case ($M_c \approx 1.0$–1.6 GeV) is marginal; perhaps charm can be used as a bridge between perturbative and nonperturbative QCD?

A set of diagrams for $b\bar{b}$ production is shown in Fig. 21.

The leading order diagrams, $O(\alpha_S^2)$ (two strong vertices), are $q\bar{q}$ annihilation to a massive virtual gluon, or $gg \to Q\bar{Q}$ with t-channel Q exchange. Higher order diagrams are gluon splitting $g \to Q\bar{Q}$, in which the $Q\bar{Q}$-pair will be close in $\eta\phi$ (probably in the same jet), flavor excitation in which only one of the $Q\bar{Q}$-pairs is at high p_T, and hard gluon radiation off any parton line.

What experimental techniques are used to study b production? The b-quark lifetime is *much* longer (about 10^{-12} s) than the formation time of hadrons (about 10^{-23} s). The b quark therefore emerges from the interaction in a hadron (B). The "average flight path" $c\tau$ for B mesons is about 460 μm, so a high-p_T B meson with a γ-factor E/M frequently travels a few mm before it decays. High-precision tracking close to the interaction point, usually with silicon strips (as in the CDF Silicon VerteX detector SVX) can reconstruct these secondary vertices and kill the overwhelming combinatorial background one would otherwise have. One can inspect the $c\tau$ distributions for prompt, charm, and bottom components and select the latter. This can be done, for b quarks, with a typical efficiency of around 30%. Another technique for tagging b hadrons or c hadrons is to use their semileptonic

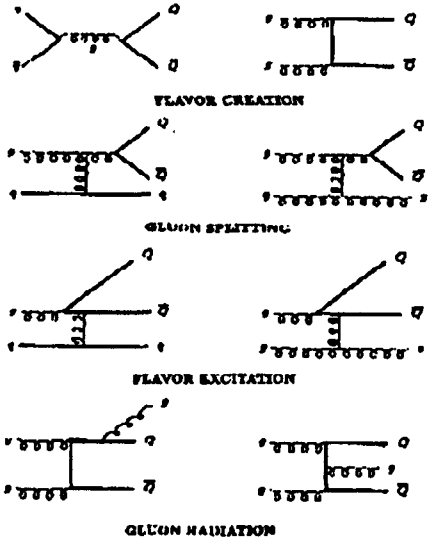

Figure 21: Feynman diagrams for leading and next-to-leading order b-quark production. Please attribute the fuzziness to quantum fluctuations!

decays. The branching fraction is about 10% to each lepton. (Of course, this is the same as for W; indeed, the process is $b \to Wc$ where the W is virtual, followed by the virtual W decay.) It is hard to use τ, but high p_T electrons or muons in or close to a hadron jet and coming from within mm of the interaction vertex make a good signature for c or b decays. Distinguishing c from b is not easy [they have similar branching fractions to leptons as you would expect, and the lifetimes are not *greatly* different: $c\tau(D^{\pm}) = 317$ μm, $c\tau(D^0) = 124$ μm, $c\tau(B) = 465$ μm]. However, the more massive b quark kicks the lepton out with larger Q than the c quark does, and this kinematic difference is quite powerful for c/b discrimination.

Figure 22 shows CDF data[34] on the production cross section for B hadrons in the central region, $|\eta| \leq 1.0$ as a function of p_T. Three different techniques were used: two look for high-p_T muons with a nearby reconstructed charmed meson (D^o, D^{*+}) and the other uses a high p_T ψ as seen in $\mu^+\mu^-$, together with a K or K^*. The latter mode has only about a 1% branching fraction—it occurs through $b \to$ "W"c followed by "W" $\to \bar{c}s$ and the c and $\bar{c}$ make a ψ—but it has a good signature. In fact, 20% of all $p_T > 5$ GeV/c ψ come from b decay. The data on B production is higher than the theory prediction by a factor three to four, more than the systematic errors on the theory (dashed lines). Experiment DØ sees a similar (although less significant) discrepancy.

If we study J/ψ production from any source (prompt, b decays, χ decays), the data is also a factor of several times higher than the predictions. To investigate this, we can separate the components. Displaced vertices in the CDF SVX select the component from b decays, which is found to be 20% for $p_T > 5$ GeV/c. The other J/ψ are "prompt," with the decay muons apparently coming from the production vertex. These can again be separated into J/ψ coming from χ decay: $\chi \to \psi\gamma$, by looking for an associated photon in the electromagnetic calorimeter with acceptable combined masses, or not coming from χ. The surprising result is that the rate of prompt ψ and ψ' production is much larger than the theoretical expectation, in the case of ψ' by a factor of 50! Here is a good example of experiment telling theory that some aspect of the theoretical calculations was badly wrong! A factor of about 50 wrong! The simplest explanation is probably that the theoretical calculations assumed that to make a J/ψ, you have to produce a c and $\bar{c}$ in a color singlet state, with the right spins and orbital angular momenta. This is asking quite a lot! Perhaps instead one can produce a c and $\bar{c}$ in any color state, e.g., color octet, and the color can be radiated away by soft gluons (which

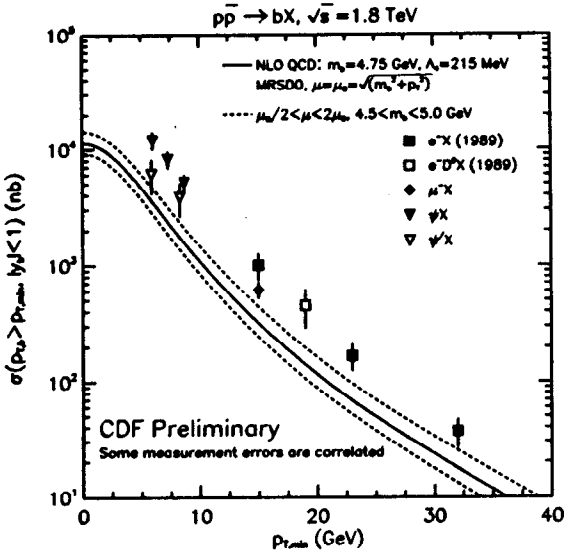

Figure 22: Cross section for B-hadron production vs p_T at the Tevatron.

is difficult to calculate) until the $c\bar{c}$ pair is colorless. Similarly, angular momenta can be radiated away until we get to the ground state. This is the *color octet model*, and it seems to do a good job of calculating the spectrum shape, but does not have much to say about the normalization (except that it should be much higher than the old *color singlet model*). One interesting test will be to study the nearby hadron density. The isolation of the J/ψ should be less in the color octet model, but being a nonperturbative effect, there are no precise predictions.

Data on open charm production at the Tevatron are meager, but as described above, the hidden charm $c\bar{c}$ sector is very interesting. What about hidden beauty, $\Upsilon(b\bar{b})$? Figure 23 shows the nicely separated peaks in the dimuon spectrum for $\Upsilon(1S), \Upsilon(2S)$, and $\Upsilon(3S)$. The Υ are all prompt; they can be decay products of excited states like χ_b, but these are prompt decays. Again, we can get a handle on them by looking for associated photons (direct photon detection capability is very useful!). The data are about an order of magnitude higher in cross section than the predictions of the color singlet model, see Figs. 24 and 25. Color octet production may account for the discrepancy.[35]

The trend towards improved agreement between theory and experiment as M_Q increases continues to the top quark. Figure 26 shows a comparison between predictions and CDF data, which are at most a factor of two higher (about 1.5 standard deviations) while DØ data agree with theory. Now we only have to consider open top production; the top quark lifetime is so short that it decays before it can form bound states. There are no top hadrons. At the Tevatron, $t\bar{t}$ pairs are produced mostly by $q\bar{q}$ annihilation. At LHC, $M/\sqrt{s}$ is seven times lower, therefore so is the x of the incident partons, and $gg \rightarrow t\bar{t}$ is dominant.

I finish this section with the search for the six-jet decays of $t\bar{t}$, which is very difficult given the large QCD six-jet background. The CDF analysis[32] selected events with six jets above 15 GeV in E_T, central, and required at least one of the jets to be b-tagged. This, of course, kills a lot of the background, which is then of a similar magnitude to the signal. One fits all jet combinations to the hypothesis

$$M_1 + M_1 \rightarrow (M_W + b) + (M_W + \bar{b}) \rightarrow (J + J)_W + b + (J + J)_W + \bar{b} \qquad (13)$$

with the two jets from each W constrained to have the right mass. M_1 is left as an unknown. The jet combination with best χ^2 is chosen, and the mass M_1 plotted in Fig. 27. The data by themselves could hardly be taken as evidence for top, so this is not a discovery channel. However, our QCD studies give us confidence in the

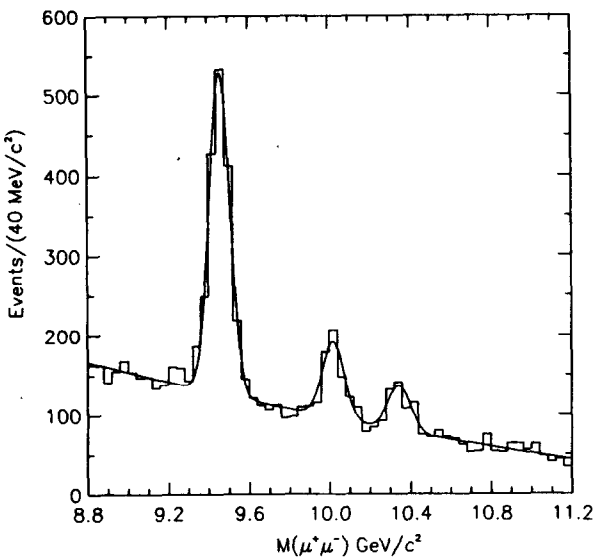

Figure 23: The dimuon $\mu^+\mu^-$ mass spectrum in CDF showing the $b\bar{b}$ resonances $\Upsilon, \Upsilon', \Upsilon''$ on top of a smooth background.

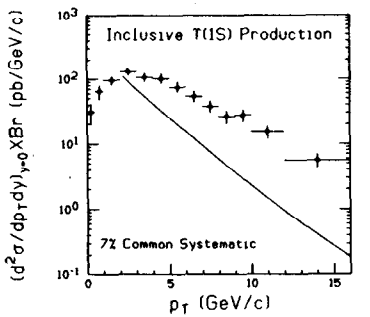

Figure 24: The cross section × branching fraction to $\mu^+\mu^-$ of the Υ compared with a QCD calculation.

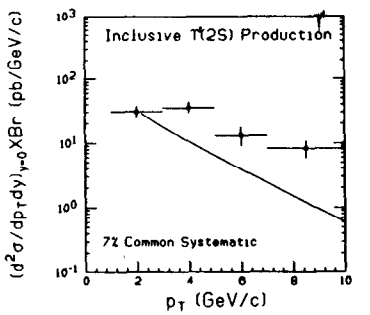

Figure 25: The cross section × branching fraction to $\mu^+\mu^-$ of the $\Upsilon'(2S)$ compared with a QCD calculation.

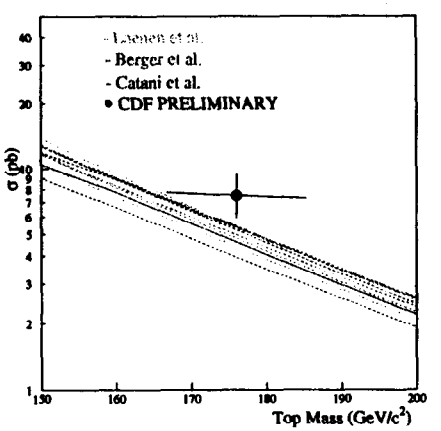

Figure 26: The cross section for production of the top quark as a function of the assumed mass M_t, together with the central value of the CDF M_t measurement and some theoretical predictions.

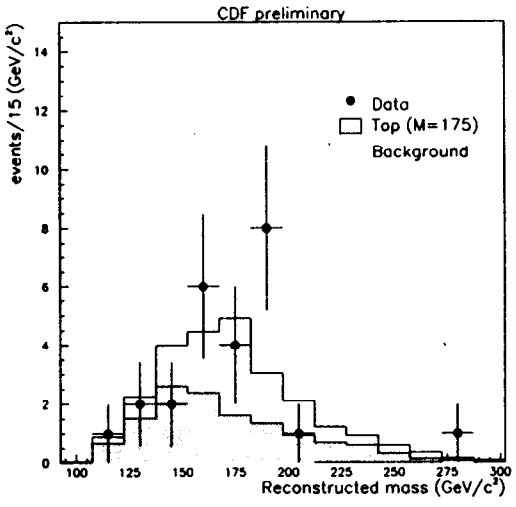

Figure 27: Six jet events (including b jets) treated as $t\bar{t}$ candidates, plotted as a function of the fitted mass M_t. The shaded area is the expected QCD $\rightarrow$ 6 jets background, and the open area the fit to a top contribution.

estimate of the non-top background, and the excess can be used to measure both M_t and $\sigma_{t\bar{t}}$ which are consistent with (but have larger errors than) measurements in the other channels.

8 Double Parton Scattering

All the hard process cross sections discussed so far have depended on the single parton distribution functions, and have ignored possible correlations between partons. The basis of the parton model is that they are non-interacting, but of course, this is not true in QCD. There are still some "trivial" correlations such as: (1) $\sum x = 1.0$ so if you find a parton with $x = 0.6$, there will be no others with $x \geq 0.4$. (2) The cloud of partons which constitute a proton has a limited radial distribution. Measuring the probability of *Double Parton Scattering, DPS,* where two independent hard scatters take place in the same $p\bar{p}$ collision, gives information on this spatial extension in the transverse plane. Obviously, the probability of a second hard scattering, given a first, will be small if the parton cloud is large, and greater if it is small. We can write schematically:

$$\sigma_{DP} \equiv \frac{\sigma_A \sigma_B}{A_{eff}}. \tag{14}$$

σ_A and σ_B are the cross sections for the two single hard scatterings, and σ_{DP} is the cross section for both in a single interaction. A_{eff} is a parameter with dimensions of area; the smaller A is, the more compact is the parton cloud and the larger the rate of double parton scattering. Commonly, σ_{eff} is used for the area A_{eff} but could be confusing as we are used to σ meaning a cross section and to event rates rising with σ rather than the inverse. So I prefer A_{eff}.

The first measurement of DPS was a study by the Axial Field Spectrometer[36] which selected events with four jets with $E_T(jet) \geq 4$ GeV and $\sum E_T(jet) \geq 25$ GeV. A jet threshold of only 4 GeV is dangerously low, but not as shocking at the ISR ($\sqrt{s} = 63$ GeV) as it would be at collider energies ten to 30 times higher. The background to DPS is "double bremsstrahlung," DBS, where a $2 \rightarrow 2$ hard collision is accompanied by radiation of two gluons. DPS and DBS are statistically distinguishable because in DPS, one pair of jets tends to balance (same E_T, opposite in ϕ) and so does the other pair, while in DBS this is not normally the case. Distributions of an *imbalance parameter* are best fit by a mixture of the processes, and from the amount of DPS, one could derive an effective radius of the

proton's parton cloud to be 0.3 fm. The fraction of four-jet events which are DPS falls rapidly with the E_T of the jets, but close to the lower cuts in the AFS data was as high as 60%. Large $\sum E_T$ triggers at fixed target energies $\sqrt{s} \leq 30$ GeV never showed the dominance of a two-jet structure, probably because with a steeply falling x distribution and parton scattering cross section, it was easier to get large $\sum E_T$ by DPS and TPS (Triple Parton Scattering) events. On the other hand, if one requires four *large* E_T jets as done by UA2 (Ref. 37) (15 GeV) or CDF[38] (25 GeV), the DPS fraction is very small. UA2 gave only an upper limit, while CDF found a signal at the significance level 2.7 σ, 5.4% for DPS/DBS.

The DPS fraction will rise strongly as the jet E_T threshold is decreased, both because of the structure function rising and because the partonic cross sections rise. CDF has a new analysis[39] which requires exactly three jets with $E_T > 5$ GeV and a direct photon candidate (it could be a π^o) above 16 GeV. Starting as low as 5 GeV was shown to still give good behavior, e.g., in terms of di-jet balancing, so the parton-jet relationship seems still to be acceptable. Having a photon (or narrow em jet) as one of the "jets" has advantages despite the lower rate. Perhaps more important, the cuts allow the two jet pairs to have rather different E_T, which reduces the allowed combinations in the $2 \times (2 \rightarrow 2)$ reconstruction. It is found that about half the events in this sample are DPS; the significance of the signal is not in doubt. Figure 28 shows the distribution of ΔS, the azimuth angle between the jet pairs, the pairs being chosen to have the best balance. This is very peaky (at $\Delta S = \pi$) for DBS but is rather flat for DPS. The area parameter is measured to be $A_{eff} = 14.5 \pm 2.6$ mb, significantly larger than the AFS result. Although we might expect A_{eff} to be rather independent of $\sqrt{s}, x$, etc., there can be some dependence. It would be interesting to have more information on this process. In fact, with the right selections, even TPS $= 3 \times (2 \rightarrow 2)$ should have a good signal:background (e.g., events with two jets above 25 GeV, two with E_T = 15 GeV–25 GeV and two with E_T = 7 GeV–15 GeV. (The staggering in E_T is, of course, just to reduce background; events with six jets above 7 GeV will have a much larger TPS signal but much larger $2 \rightarrow 6$ background.)

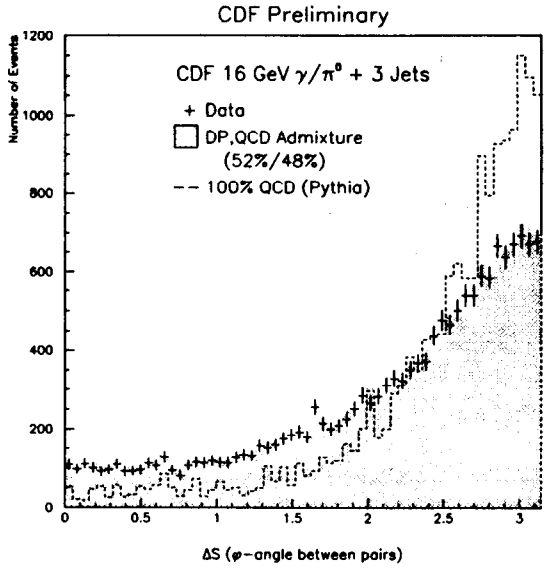

Figure 28: The azimuth angle is plotted between the best balancing pairs in γJJJ events. Double parton scattering gives a flat distribution.

9 Color Coherence

Among the other interesting phenomena which are being studied at the Tevatron, *color coherence* deserves attention. A proper simulation of strong interactions

would compute all the color wavefunctions in space-time, and derive probabilities of finding particles by adding and then squaring the wavefunctions. As in optics, we have destructive or constructive interference, giving rise to "fringes" or at least angular regions that tend to be depleted or enhanced (extremely broad fringes if you like). We do not generate our Monte Carlo events at this level, but the effects of this color coherence can be seen. One manifestation is a *string effect* in $e^+e^- \to q\bar{q}g$ three-jet events where some angular regions get enhanced, others depleted. Another is *angular ordering* in a parton cascade, where successive opening angles are progressively smaller ($\theta_1 \geq \theta_2 \geq \theta_3$, etc.). As usual, $p\bar{p}$ interactions are more complicated than e^+e^- because we have gluon radiation in both the initial and final states, and interference occurs between them. Some Monte Carlo programs include angular ordering effects [HERWIG, PYTHIA+, PYTHIA5.6 (final state only)] and others (ISAJET, JETRAD) do not. One can look[40] at events with one stiff leading jet (Jet1) and two others (Jet2, Jet3). Jet3 is normally near Jet2, and we can plot its distribution around Jet2 as an angle in the η, ϕ plane. Preliminary data from DØ show that the third jet is much more likely to be between Jet2 and the beam directions than orthogonal (i.e., at the same η as Jet2). HERWIG seems to get this right while ISAJET (with no color coherence) does not.

10 Jet Fragmentation

Studies of jet fragmentation have received a lot more attention recently at LEP,[4] from $e^+e^- \to q\bar{q}$, than at the Tevatron. It is an interesting arena for pushing QCD to its soft limits, and understanding how a hard quark in a color field transforms into isolated colorless soft hadrons. Modeled as a branching tree of quarks and gluons, one has to handle the problems of α_S diverging as four-momenta Q become smaller, giving so-called *soft divergences* and *colinear divergences*. (These are not important for a calorimetric jet measurement, but here we are discussing the hadronic structure.) One normally puts a cut-off scale Q_0 of several GeV on the cascade, to keep emission probabilities small:

$$w \approx \alpha_S \cdot ln^2 \frac{E}{Q_0} \cdot \tag{15}$$

In the 1970s and 1980s, tools for summing divergencies were developed especially by the "Russian school"[41] which led to the Leading Log Approximation, LLA, and recently to the Modified LLA or MLLA by Mueller,[42] Dokshitzer, and Troyan.[43] This results in a formula for jet fragmentation into hadrons with essentially only two parameters, an effective cut-off Q_{eff} of the parton cascade and the ratio of hadron multiplicity to parton multiplicity (at the cut-off scale). Color interference, giving angular ordering, is incorporated. The MLLA manages to get very reasonable fits to many fragmentation variables. One such is the variable

$$\xi = ln\frac{1}{z} \tag{16}$$

where

$$z = \frac{p_{had}}{p_{JET}} \tag{17}$$

is the fractional momentum of the hadron along the jet axis. $\xi = 0$ then corresponds to a single hadron jet, while a soft hadron with $z = 0.0025$ has $\xi \approx 6$. In a CDF study,[44] all the charged hadrons within a cone around the jet axis of radius 0.466 rad are counted, and the ξ distributions are plotted in Fig. 29 for several values of the leading dijet mass from 105 to 625 GeV. Good fits are obtained to a form derived from the MLLA. Surprisingly, the parameter Q_{eff} for these fits is very low, about 240 MeV, but this should not be interpreted as "QCD works down to 240 MeV." However, the parameterizations given by the MLLA methods can apparently be extrapolated with some success even down to this soft region.

Studies show that the cone size θ can be varied and the fits remain good with stable parameters. The position of the peaks in Fig. 29 depend both on E_J and θ, but it is just the product $E_J\theta$ which matters. If we define

$$Y = ln\frac{E_J\theta}{Q_{eff}}, \tag{18}$$

then the position ξ_0 of the peak is given by

$$\xi_0 = \frac{1}{2}Y + \sqrt{cY} - c, \tag{19}$$

where c is a constant; 0.292 fits the data. We then can show a universal curve of ξ_0 versus $M_{JJ}\theta$ with CDF points for several dijet masses together with LEP e^+e^- data, see Fig. 30. This emphasizes the similarity of the internal structure of jets at the Tevatron ($p\bar{p}$) and LEP (e^+e^-).

11 Diffraction and Rapidity Gaps

Essentially everyone agrees that QCD is The Theory of Strong Interactions. Nevertheless, we actually know how to calculate only a very small fraction of strong

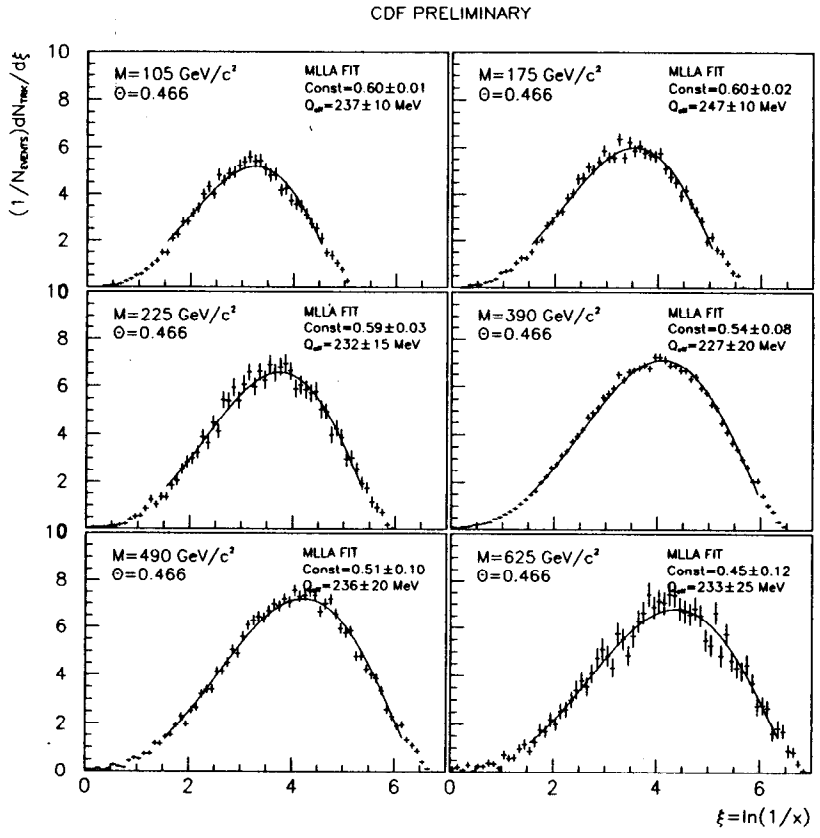

Figure 29: For six different dijet masses, the distribution of the jet fragmentation variable ξ is shown and compared to a fit derived from the MLLA formalism.

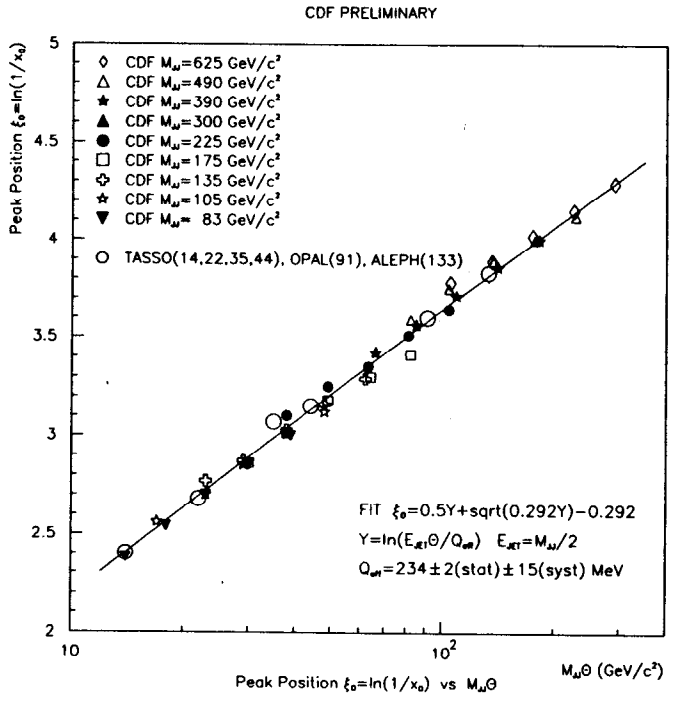

Figure 30: The jet fragmentation parameter ξ_o vs $M_{JJ}\theta$ for Tevatron and LEP jets.

interaction physics (large Q^2) and therefore do not have a good understanding of such "soft" phenomena as the total cross section σ_T, elastic scattering $\frac{d\sigma}{dt}$, diffractive dissociation, and double Pomeron exchange. The *Pomeron*, $I\!P$, can be defined[46] operationally as the dominant strongly interacting entity exchanged over large rapidity gaps. In elastic scattering at the Tevatron, the p and $\bar{p}$ are separated by 15 units of rapidity, and the four-momentum transfer exchanged is carried by the Pomeron, except at very small t where photon exchange dominates *(Coulomb scattering)*. The imaginary (absorptive) part of the elastic scattering amplitude at $t \to 0$ is proportional to the total cross section σ_T; this is the famous optical theorem. The Pomeron therefore "drives" the total cross section. Regge theory is not much taught now, but it is more successful than QCD at "explaining" much soft strong interaction data. Could it one day be "derived" from QCD? In Regge theory,[45] Pomerons and other *Reggeons* are exchanged carrying complex angular momentum $\alpha(t)$. At any t, the highest α tends to dominate, and at $t \approx 0$, this is the Pomeron. Total cross sections behave like:

$$\sigma_T = C \cdot s^{\alpha_{I\!P}(0)-1}, \tag{20}$$

so as $\alpha_{I\!P}(0)$ exceeds 1.0 total cross sections rise with energy $\sqrt{s}$. In fact, a more theoretical definition of the Pomeron[46] is: "The highest Regge trajectory, with the quantum numbers of the vacuum, responsible for the growth in hadronic total cross sections at high energy." It has the quantum numbers of the vacuum (zero I-spin, no charges), which is not surprising as a proton can "emit" a Pomeron and remain a proton. The relation between the Pomeron and the QCD vacuum (gluon condensates?) is interesting. So now I have defined it (twice!), but what is it? QCD has quark and gluon fields, so presumably the Pomeron should be describable in the same terms.

There is currently much progress in trying to understand the Pomeron by studying hard diffractive processes, i.e., events with both a Pomeron and a large Q^2 process such as high E_T jet production or W production. The idea is to think of the Pomeron as a *quasiparticle*. Think of it as a particle, Pomeron ($I\!P$) that can be emitted with some flux and absorbed, and that has a structure function $g_{I\!P}(\beta, Q^2, t)$ and $q_{I\!P}(\beta, Q^2, t)$ where β is the fraction of the Pomeron momentum carried by the parton. This may not be a very sound theoretical concept but it seems to work, and by trying to measure the Pomeron partonic structure in different processes, we put it to the test.

11.1 Jet-Gap-Jet Events

In 1993, Bjorken predicted[47] that hard scattering between two partons, leading to two high E_T jets, could occur not only by gluon or quark exchange but also by a color singlet exchange, most simply by two-gluon exchange with gluons of opposite color. In the early days of QCD, Low[48] and Nussinov[49] had proposed that the Pomeron is two gluons. Because no color is exchanged between the right-moving and left-moving systems, there is no color field between them and hadrons are not formed; hence we should have a rapidity gap, defined as a region of rapidity containing no particles. To be dominated by color singlet exchange, rather than just a fluctuation in the rapidity separations of particles in a normal "non-diffractive" event, the rapidity gap Δy should be larger than about three units. Bjorken could calculate the probability for the two-hard-gluon exchange, but could only estimate the probability that the rapidity gap would not be spoiled by some additional soft color exchange in the event. This he called the *Survival Probability*, S, and estimated it to be about 10%, leading to an expected fraction of events with gaps between jets in the range $0.003 < R_{gap} < 0.03$. Both DØ and CDF found[50,51] such events at a level near 1%. One technique is to select events with two forward jets on opposite sides ($\eta_1\eta_2 < 0$) and to count charged hadrons in a central rapidity region $-1 < \eta < 1$. Figure 31 shows such a plot (solid line) compared with the multiplicity distribution when the two jets are on the same side ($\eta_1\eta_2 > 0$). An excess is seen in the bin of zero tracks, at the level of $(1.13 \pm 0.16)\%$. It is interesting to know whether this gap fraction depends on the E_T and/or η of the jets, and also whether, if we could discriminate between quark and gluon jets (not easy), the q/g mix is the same for gap and nongap events. The point is whether the hard color singlet exchange differentiates between quarks and gluons. Between about 20 GeV and 45 GeV, CDF sees[52] no significant change in the gap fraction with E_T, while DØ sees an increase, from 18 GeV to 50 GeV, from 0.4% to 1.4% (Ref. 53). However, the errors on both measurements are such that the data are not in significant disagreement and more study is required. The same statement is true for the dependence of the gap fraction on rapidity separation between the jets; CDF sees a hint of a decrease in gap fraction at the largest $< |\eta| >$ (3.0–3.4) which is not seen by DØ. These issues should be resolved, and we should extend the data to lower E_T and eventually study the transition to

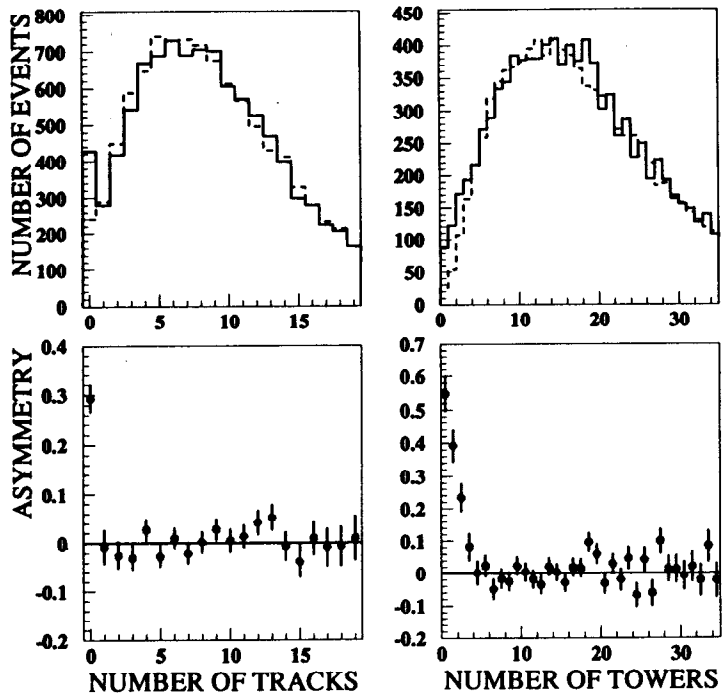

Figure 31: Track (left) and calorimeter tower (right) multiplicity distributions (top) in the central region ($|\eta| < 1$) between two high-p_T (> 25 GeV) jets (solid lines, OS jets). The dashed lines show the same when the two jets have the same rapidity, far from the central region (SS jets). The bottom figures show the difference (OS-SS)/SS with the evidence for a rapidity gap.

double diffractive dissociation without jets, a subject not yet properly studied at colliders.

Another topic for future study, but which will probably be difficult, is that of rapidity gaps with double parton scattering. The idea is to select events with two jets at large positive rapidity and two at large negative rapidity, use the pairwise balancing techniques discussed above to select a DPS component, and then look for rapidity gaps in the center. We should learn something about the dynamics of the color singlet exchange.

11.2 Single Diffractive Excitation

While the events with gaps between jets were first published[50] only two years ago, single diffractive excitation has a long history. Before the ISR started in 1971, it was known that an incident hadron could be excited into a low mass resonance with the same quantum numbers, and the cross section stays up as the energy increases. Good and Walker[54] (experimentalists!) had much earlier proposed this phenomenon. Their mechanism was basically that the beam particle is actually a superposition of virtual states ($p/n\pi^+/p\pi^+\pi^-/\Lambda K^+$/etc.), which are differentially absorbed by the target so the beam "particle" can emerge in a different state. This was an s-channel, optical model viewpoint which went out of fashion in favor of the t-channel Pomeron, but Bjorken[55] is advocating its revival.

In 1973, experiments at the ISR found that the range of diffractive masses scales with $\sqrt{s}$, extending to about 14 GeV there, and later at the CERN $Sp\bar{p}S$ Collider to 140 GeV. The $Sp\bar{p}S$ was therefore in the energy regime where high-p_T jets might be seen also in diffractive events. Ingelman and Schlein[56] proposed that such events could be considered as Pomeron-proton collisions, and thus by measuring jets, we could learn about the parton structure of the Pomeron. Schlein and collaborators installed "Roman pots" (special vacuum pots with detectors to measure protons scattered at very small angles and with nearly the full beam momentum, see Fig. 4, first used by the CERN-Rome Collaboration at the ISR) next to the UA2 detector which was used to look for jets. They found such events, with two jets above 7 GeV, and from the E_T and η distribution of the jets, they concluded that the parton distribution in the Pomeron is rather hard, like $\beta(1-\beta)$ where $\beta = p_{parton}/p_{I\!P}$. They also claimed a "superhard" component with a single parton carrying nearly all of the Pomeron momentum, but smeared by resolution

and acceptance effects. This would be very interesting, suggesting a picture of the Pomeron behaving like a single hard gluon with its color "bleached" by a soft gluon cloud. Data from H1 at HERA[57] also derive a structure of the Pomeron at very low Q^2 which is a quasi-δ-function gluon at $\beta \approx 1$. This is not directly measured but inferred from the pattern of scaling violations in the quark structure. Even at very high β, the quark density rises with Q^2, so it must be fed by gluons at even higher β. If the Pomeron really appears to be a single high-β gluon with an accompanying soft cloud, that would be very strange. According to Alan White[58] "gauge invariance requires that all the gluons in a color zero vacuum exchange are identical." His solution to this dilemma is to introduce a quantum number: *color charge parity* C_c. The hard and soft gluons carry different values of C_c.

Recently, both CDF and DØ have also found diffractively produced dijets. The method is to select events with a pair of jets at similar forward η (SS = Same Side, $|\eta| > 1.8$ or so) and to look at the multiplicity distribution (calorimeter towers or tracks) on the far opposite side, say $2 < \eta < 5$. This distribution shows[59,60] a distinctive spike in the zero-multiplicity bin which is the diffractive signature, at the level of 0.7% of the dijet sample. CDF also had Roman pot detectors located 57 m downstream along the outgoing $\bar{p}$ pipe and took data with the diffractively scattered $\bar{p}$ detected. This tags the mass of the $I\!Pp$ system and measures the t of the Pomeron. Jets are observed; the data are still being studied, and it will be interesting to compare with the UA8 studies and look for the "δ-function" component.

11.2.1 Diffractive W Production

The study of diffractive dijets tells us about the Pomeron structure but without distinguishing between quark and gluon constituents, both of which produce jets. Experiments at HERA on diffractive DIS probe the Pomeron with photons and hence select the quark component. In hadron colliders, one can look for Drell-Yan lepton pair production, $q\bar{q} \to l^+l^-$, $W^\pm$, or Z production to probe the quarks. CDF have now done this[61] and find that (1.15±0.55)% of all W are diffractively produced at the Tevatron. This is very much less than one particular prediction[62] which said that *if* the Pomeron were only $q\bar{q}$, as much as 15%–24% of all produced W could be diffractive. How could it be so high, when the total diffractive cross section is only about 10% of the total cross section? The answer might be that the Pomeron is more efficient than the proton at producing W (on another proton) as it is smaller ($\sigma_{I\!Pp} \approx$ few mb), but the partonic cross sections are the same.

We can now put four *diffractive* results together: DIS cross section at HERA,[63] jet production at HERA, jet production at the Tevatron, and W production at the Tevatron, to see whether we get a consistent picture for the Pomeron. We can choose as two parameters $\Sigma_{I\!P}$, the momentum fraction of the Pomeron carried by hard (participating) partons, and $g_{I\!P}$, the fraction of those hard partons which are gluons. The form $\beta(1-\beta)$ is assumed. Each of these results constrains us to a band in the plane $(\Sigma_{I\!P}, g_{I\!P})$, processes favoring quarks going up to the right, and processes favoring gluons going up to the left, see Fig. 32.

The intersections of these bands are the favored regions (at the 1σ level). Both ZEUS and CDF favor $g_{I\!P} \approx 0.5$–0.7 but differ in the estimate of $\Sigma_{I\!P}$. We could be seeing here a breakdown of factorization, or a breakdown of the (perhaps naïve) picture of the Pomeron as a quasiparticle with a structure function, or an indication that the Pomeron *flux* is not correctly calculated. Goulianos has proposed[64] the latter solution, suggesting that the Pomeron flux from high energy hadrons must be renormalized such that it never exceeds 1.0 (otherwise the diffractive cross sections become large, even compared to the total cross sections). This may bring ZEUS and CDF $\Sigma_{I\!P}, g_{I\!P}$ values into agreement, although it is not clear how the ZEUS data should be renormalized, and of course, we need better data. Schlein has also recently proposed[65] a Pomeron flux renormalization but not global (like Goulianos), but preferentially damping small $\xi = 1 - x_F$ values.

The use of the parameters $\Sigma_{I\!P}, g_{I\!P}$ is one way of treating data which is not good enough to properly measure the full structure functions $g_{I\!P}(\beta, Q^2, t)$ and $q_{I\!P}(\beta, Q^2, t)$; this is our ambition but it needs very high statistics. As previously stated, H1 and ZEUS at HERA are measuring $q_{I\!P}(\beta, Q^2)$, and H1 suggest that it may derive from what looks like (90%) a single gluon at low Q^2, rapidly evolving into a q/g mixture.

11.2.2 Double Pomeron Exchange

Finally, a few words about the reaction called *Double Pomeron Exchange*. A Pomeron is emitted from each incident hadron, the hadrons scatter quasielastically, and the two Pomerons interact in the central region. The final state has the two beam particles with x_F greater than about 0.95, followed by rapidity

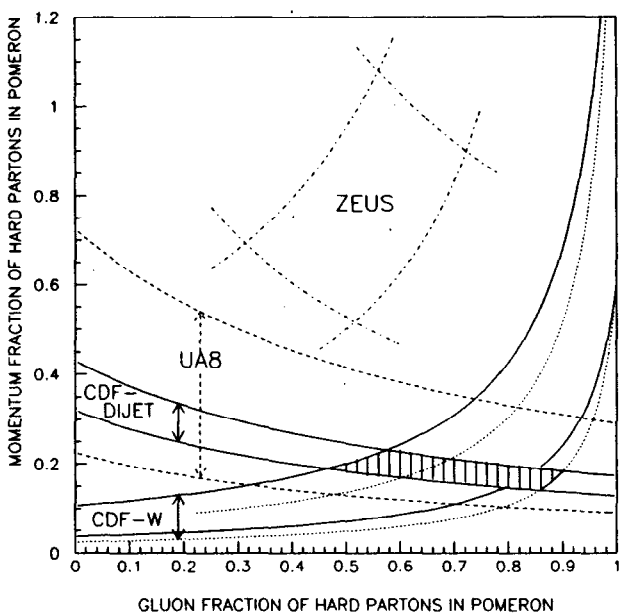

Figure 32: Allowed areas in the plane $\Sigma_{I\!P}$, the fraction of the Pomeron momentum carried by hard partons, and $g/I\!P$, the fraction of hard partons which are gluons. The CDF W and JJ production constrain the region to the hatched area; ZEUS data imply a larger $\Sigma_{I\!P}$.

gaps of three or more units, and central hadrons, with central mass $M_\odot$. The rule of thumb relation, for which double Pomeron exchange dominates over other exchanges (e.g., Pomeron-Reggeon), is

$$M_\odot < 0.05\sqrt{s}, \tag{21}$$

which means:

- 3 GeV at the ISR (hadrons, glueball spectroscopy[66]),
- 90 GeV at the Tevatron (high E_T jets),
- 700 GeV at the LHC (W? H? *SUSY*?).

Double Pomeron exchange is still very little studied at the Tevatron, and not much was done at the $Sp\bar{p}S$ Collider either,[67,68] but it could be very interesting. The rate of double Pomeron events should help resolve issues about Pomeron flux renormalization. Hard scattering dijet events should be sensitive to the question of a δ-function gluon, through observing events where the central system is just two jets (like an e^+e^- event, but from gg!). It should be noted that the interesting LHC process of Higgs production via $W^+W^- \to H^0$ fusion also can leave rapidity gaps, since the W's are colorless. $I\!P I\!P$ processes can be a background to this. However, any processes with rapidity gaps will be difficult to study in the big "high mass" experiments ATLAS and CMS because they require single interactions and therefore modest luminosity. The FELIX experiment will cover this field better, with very large rapidity acceptance and deliberately modest luminosity.

12 Concluding Remarks

I hope I have communicated a sense that hadron-hadron colliders are a gold mine for QCD studies and a great deal is going on. Of course, a glance at these proceedings will show that e^+e^- and ep collisions are also great places to study QCD, and the three types of colliders complement one another nicely. Nearly everyone now agrees that **QCD is the theory of strong interactions**. Nevertheless, QCD being "right" does not mean that there will be no more surprises. On the contrary, we saw that prompt J/ψ are being produced at a rate about *50* times higher than anticipated. From this, we are learning about the subtle behavior of color in a soft, nonperturbative regime. B-quark production is higher than predicted by a

factor of a few, and $t\bar{t}$ production by a factor less than about 50%. Searching for new physics beyond the Standard Model often demands excellent understanding of QCD. Even more challenging is the fact that high cross section processes like diffraction dissociation, elastic scattering, and the total cross section itself are not yet calculable and therefore not yet well-understood. It is very exciting that we are now learning to extend the domain of calculability of QCD to phenomena such as very low-x partons, the Pomeron, and other color magic. I am reminded about other fields of physics, where collective phenomena like superfluidity and superconductivity were not predicted from basic atomic theory and Quantum Mechanics but were experimental discoveries. Perhaps there are exciting new strong interaction phenomena just waiting to be found!

Acknowledgments

I am aware that I have not kept a fair balance between different experiments. I hardly mentioned the major experiments UA1 and UA2 at the CERN $Sp\bar{p}S$ Collider, and most of my illustrations were from CDF rather than DØ. I apologize, but only a little; these lectures were meant to be pedagogical and not to be a review.

I would like to thank Steve Behrends and Dino Goulianos for comments on the manuscript; Keith Ellis, Heidi Schellman, and Andreas Vogt for some figures; and Sue, Cele, and Randy Herber for technical help with figures.

References

[1] R. P. Feynman, Phys. Rev. Lett. **23**, 1415 (1969).

[2] F. E. Close, *The Current Picture of Glueballs*, hep–ph/9610426 RAL-96-085 (1995). D. Barberis *et al.* (WA102), CERN-PPE-96-197, submitted to Phys. Lett.

[3] *The "Pipetron," a Low-Field Approach to a Very Large Hadron Collider*, edited by E. Malamud, selected papers (Fermilab, 1997).

[4] P. Burrows, lectures on "Precision Tests of QCD in e^+e^- Annihilations," these proceedings.

[5] W. Smith, lectures on "QCD Studies in *ep* Collisions," these proceedings.

[6] A. Pickering, *Constructing Quarks* (Univ. Chicago Press, 1984).

[7] L. N. Lipatov, Sov. J. Nucl. Phys. **20**, 95 (1975); V. N. Gribov and L. N. Lipatov, Sov. J. Nucl. Phys. **15**, 438 (1972); G. Altarelli and G. Parisi, Nucl. Phys. B **126**, 298 (1977); Y. L. Dokshitzer, Sov. Phys. JETP **46**, 641 (1977).

[8] E. D. Bloom *et al.* (SLAC-MIT), Phys. Rev. Lett. **23**, 930 (1969); G. Miller *et al.* (SLAC-MIT), Phys. Rev. D **5**, 528 (1972).

[9] G. Parisi and R. Petronzio, Phys. Lett. B **62**, 331 (1976). M. Glück, E. Reya, and A. Vogt, Z. Phys. C **67**, 433 (1995).

[10] A. D. Martin, R. G. Roberts, and W. J. Stirling (MRS), Phys. Lett. B **306**, 145 (1993); Phys. Rev. D **50**, 6734 (1994); Phys. Lett. B **354**, 155 (1995).

[11] J. Botts *et al.* (CTEQ), Phys. Lett. B **304**, 159 (1993).

[12] R. K. Ellis, W. J. Stirling, and B. R. Webber, *QCD and Collider Physics* (Cambridge, 1996), an excellent and up-to-date textbook.

[13] S. M. Berman, J. D. Bjorken, and J. B. Kogut, Phys. Rev. D **4**, 3388 (1971).

[14] C. Bromberg *et al.*, Phys. Rev. Lett. **38**, 1447 (1977); M. Corcoran *et al.*, Phys. Rev. D **21**, 641 (1980).

[15] T. Akesson *et al.* (AFS Collaboration), Phys. Lett. B **118**, 185, 193 (1982).

[16] T. Akesson *et al.* (AFS Collaboration), Z. Phys. C **30**, 27 (1986).

[17] M. Banner *et al.* (UA2), Phys. Lett. B **118**, 203 (1982); J. Appel *et al.* (UA2), Phys. Lett. B **160**, 349 (1995).

[18] G. Arnison *et al.* (UA1), Phys. Lett. B **123**, 115 (1983); Phys. Lett. B **172**, 461 (1986).

[19] G. Hanson *et al.*, Phys. Rev. Lett. **35**, 1609 (1975).

[20] F. Abe *et al.* (CDF), Phys. Rev. Lett. **70**, 1376 (1993). The $\sqrt{s} = 630$ GeV data are not yet published.

[21] F. Abe *et al.* (CDF), Phys. Rev. D **54**, 4421 (1996).

[22] G. Sterman, in *Proceedings of the 10th Workshop on Proton-Antiproton Collider Physics* (Batavia, 1995), hep-ph/950835.

[23] W. Giele, in *Proceedings of the 10th Workshop on Proton-Antiproton Collider Physics* (Batavia, 1995), Fermilab-Conf-95-169-T.

[24] M. L. Mangano, CERN-TH/96-278, hep-ph/9610234. "Topics in jet physics," in *Proceedings of the XI Topical Workshop on Hadron Collider Physics* (Padova, 1996).

[25] F. Abe *et al.* (CDF), Phys. Rev. Lett. **74**, 3538 (1995).

[26] E. A. Kuraev, L. N. Lipatov, and V. S. Fadin, Phys. Lett. B **60**, 50 (1975); Sov. Phys. JETP **45**, 199 (1977); Y. Y. Balitsky and L. N. Lipatov, Sov. J. Nucl. Phys. **28**, 822 (1978).

[27] S. Abachi *et al.* (DØ), Phys. Rev. Lett. **77**, 595 (1996).

[28] F. Abe *et al.* (CDF), Phys. Rev. D **54**, 4221 (1996).

[29] M. Diakonou *et al.* (R806), Phys. Lett. B **87**, 292 (1979).

[30] J. Alitti *et al.* (UA2), Phys. Lett. B **263**, 544 (1991).

[31] C. Kourkoumelis *et al.* (R806), Z. Phys. C-Particles and Fields, **16**, 101 (1982).

[32] F. Abe *et al.* (CDF), "First observation of the all hadronic decay of $t\bar{t}$ pairs," CDF/4025, submitted to Phys. Rev. Lett., March 1997.

[33] F. Abe *et al.* (CDF), Phys. Rev. Lett. **77**, 448 (1996).

[34] J/ψ and ψ' Production at CDF, FERMILAB-CONF-96/156-E, CDF Note 3721 (1996).

[35] P. Cho and A. K. Liebovich, Cal. Tech preprint CALT-68-1988, hep-ph-9505329; E. Braaten and S. Fleming, Phys. Rev. Lett. **74**, 3327 (1995).

[36] T. Akesson *et al.* (AFS), Z. Phys. C-Particles and Fields **34**, 163 (1987).

[37] J. Alitti *et al.* (UA2), Phys. Lett. B **268**, 145 (1991).

[38] F. Abe *et al.* (CDF), Phys. Rev. D **47**, 4857 (1993).

[39] F. Abe *et al.* (CDF), "Measurement of double parton scattering in $p\bar{p}$ collisions at $\sqrt{s} = 1.8$ TeV," CDF/4053, to be submitted to Phys. Rev. Lett.

[40] S. Abachi *et al.* (DØ), XVII Int. Symp. on Lepton Photon Interactions (LP95), Beijing, China, Aug. 1995.

[41] Y. L. Dokshitzer, V. A. Khoze, A. H. Mueller, and S. I. Troyan, *Basics of Perturbative QCD* (Editions Frontieres, 1991).

[42] A. H. Mueller, Nucl. Phys. B **213**, 85 (1983).

[43] Y. L. Dokshitzer and S. I. Troyan, in *Proceedings of the XIX Winter School of LNPI* **1**, 144 (1984).

[44] F. Abe *et al.* (CDF), MLLA paper in preparation.

[45] P. D. B. Collins, *An Introduction to Regge Theory and High Energy Scattering* (Cambridge Univ. Press, Cambridge, 1977).

[46] M. G. Albrow *et al.*, FERMILAB-Conf-96/377-E, in *Proceedings of the Snowmass '96 Summer Study on New Directions for Particle Physics* (1996).

[47] J. D. Bjorken, Phys. Rev. D **47**, 101 (1993).

[48] F. Low, Phys. Rev. D **12**, 163 (1975).

[49] S. Nussinov, Phys. Rev. D **14**, 246 (1976).

[50] F. Abe *et al.* (CDF), Phys. Rev. Lett. **74**, 855 (1995).

[51] S. Abachi *et al.* (DØ), Phys. Rev. Lett. **72**, 2332 (1994).

[52] F. Abe *et al.* (CDF), "Events with a rapidity gap between jets at the Tevatron," paper in preparation.

[53] T. Taylor Thomas (DØ), in *Proceedings of the Small-x and Diffractive Physics Workshop* (Argonne, Sept. 1996).

[54] M. L. Good and W. D. Walker, Phys. Rev. **120**, 1854 (1960).

[55] J. D. Bjorken, in *Proceedings of the Small-x and Diffractive Physics Workshop* (Argonne, Sept. 1996).

[56] G. Ingelman and P. Schlein, Phys. Lett. B **152**, 256 (1985).

[57] P. Biddulph (H1), in *Proceedings of the Small-x and Diffractive Physics Workshop* (Argonne, Sept. 1996).

[58] A. R. White, in *Proceedings of the Small-x and Diffractive Physics Workshop* (Argonne, Sept. 1996).

[59] S. Bagdasarov (CDF), in *Proceedings of the Small-x and Diffractive Physics Workshop* (Argonne, Sept. 1996).

[60] K. Mauritz (DØ), in *Proceedings of the Small-x and Diffractive Physics Workshop* (Argonne, Sept. 1996).

[61] F. Abe *et al.* (CDF), "Observation of diffractive W-boson production at the Tevatron," submitted to Phys. Rev. Lett. (1997). CDF-3799.

[62] P. Bruni and G. Ingelman, Phys. Lett. B **311**, 317 (1993).

[63] M. Derrick *et al.*, Phys. Lett. B **356**, 129 (1995).

[64] K. Goulianos, Phys. Lett. B **358**, 379 (1995).

[65] P. Schlein, in *Proceedings of the Small-x and Diffractive Physics Workshop* (Argonne, Sept. 1996).

[66] T. Akesson *et al.* (AFS), Nucl. Phys. B **264**, 154 (1986).

[67] D. Joyce *et al.* (UA1), Phys. Rev. D **48**, 1943 (1993).

[68] A. Brandt *et al.* (UA8), Singapore Conference (1990), "Observation of Double Pomeron Exchange. . . ."